

**PRE-FEASIBILITY STUDY REPORT
FOR
THE RIFT VALLEY GEOTHERMAL
DEVELOPMENT PROJECT
IN THE REPUBLIC OF KENYA**

JANUARY, 1983

JAPAN INTERNATIONAL COOPERATION AGENCY

国際協力事業団	
受入 月日 84.8.27	407
登録No. 08196	55.5
	MPN

PERFACE

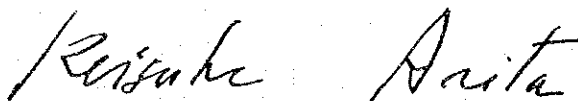
In response to the request of the Government of the Republic of Kenya, the Government of Japan decided to conduct a survey on the Rift Valley Geothermal Development Project and entrusted the survey to the Japan International Cooperation Agency (JICA). The JICA sent to the Republic of Kenya a survey team headed by Dr. Koji Motojima four times from October 1979 to December 1982.

The team exchanged views with the officials concerned of the Government of Kenya and conducted a survey on geology, rock alteration, geochemistry, geophysics etc. with a view to assessing geothermal potentiality in Eburru area, Rift Valley Province. After the team returned to Japan, further studies were made and the present report has been prepared.

I hope that this report will serve for the development of the Project and contribute to the promotion of friendly relation between our two countries.

I wish to express my deep appreciation to the officials concerned of the Government of the Republic of Kenya for their close cooperation extended to the team.

Tokyo, January 1983

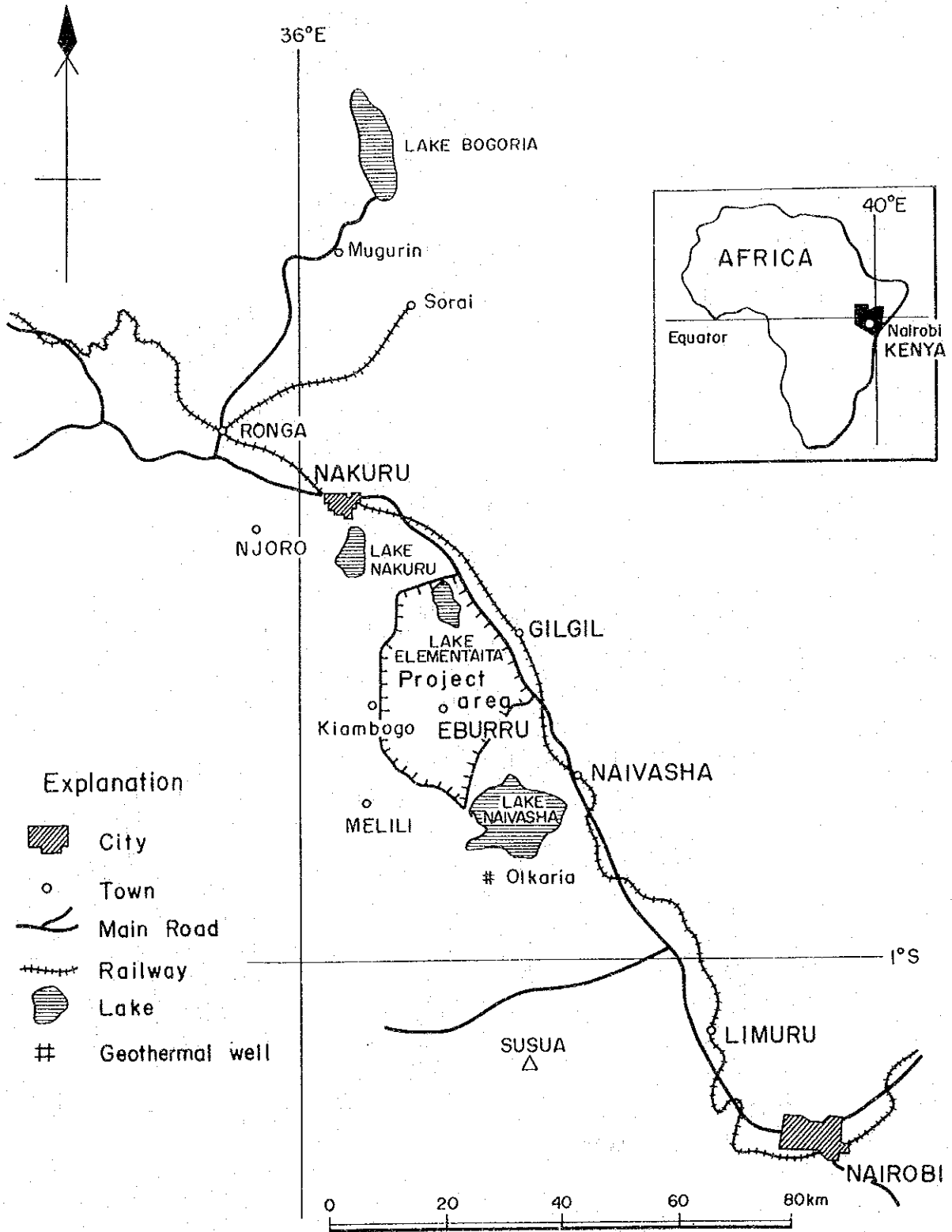


Keisuke Arita

President

Japan International Cooperation Agency

Fig. 1 Location of Project Area



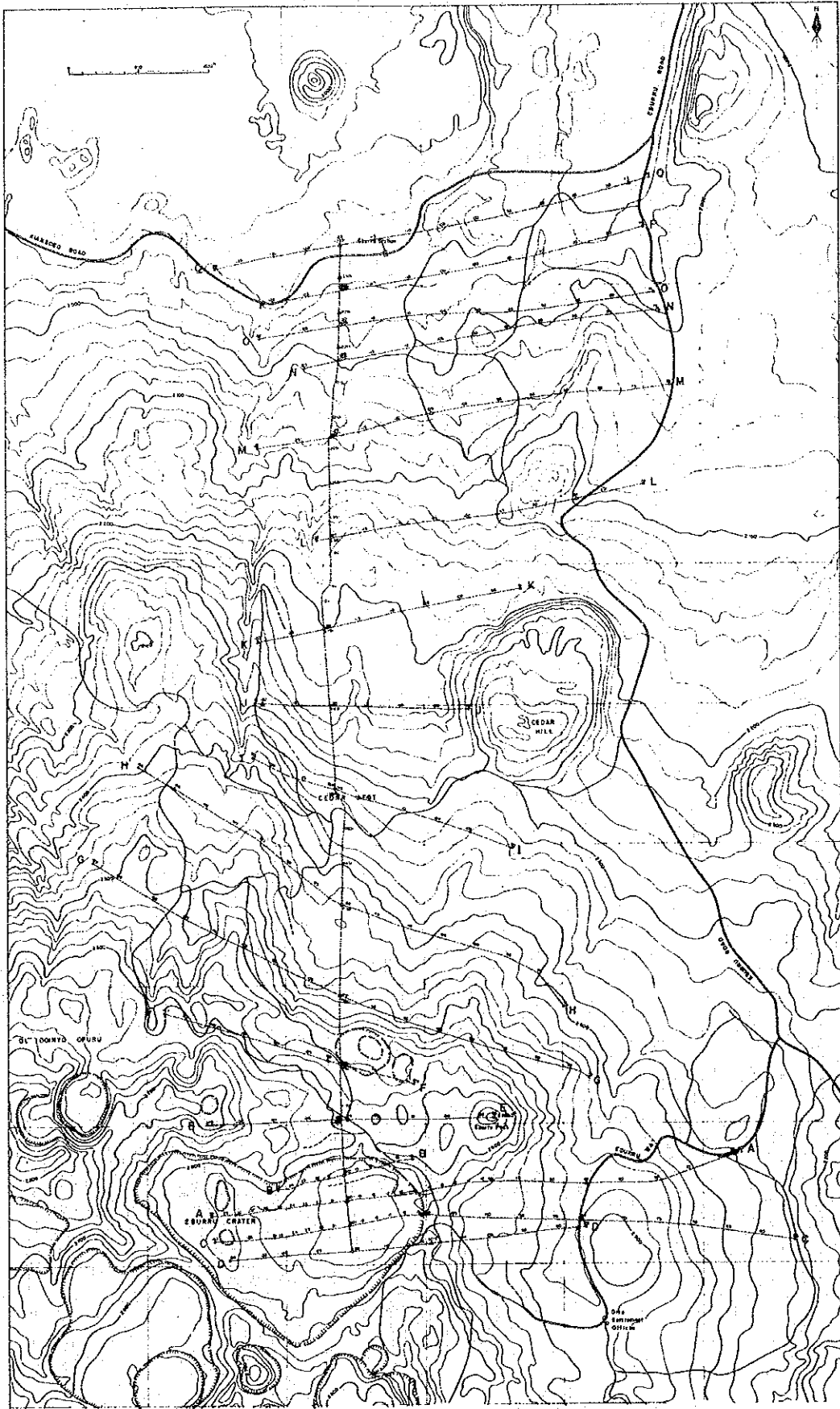


Fig. 2 Location of Project Area

CONCLUSIONS

As a result of the field survey, the rock alteration survey leads us to the hypothetical geothermal model of Eburru Geothermal system (see Fig. 5). All other field survey, 1 meter depth ground temperature, Hg distribution in soil and soil-air, CO₂ distribution in soil-air, geological survey and geoelectrical soundings support the model, therefore, we use the model as our working hypothetical model.

The hypothetical geothermal model is:

- a) Heat source of the area is under Eburru Crater extending to the east.
- b) Underground water flows from Lake Naivasha to the north.
- c) Geothermal manifestations around Eburru Crater are formed because of the heat source right underneath.
- d) Geothermal manifestations around Eburru Station are formed because the underground water table is very shallow around the area.

This model suggests that the Eburru Prospect may have very high geothermal potential.

Geology

1. The survey area is composed of erupted and ejected volcanic rocks in the Rift Valley during Pleistocene and younger age. Most of them are acidic alkaline rocks. There are no sedimentary rocks in the prospect.
2. The geological succession of the area is, from lower to upper, welded tuff, phonolite and comendite lava flow, Ol Doinyo Opor pumice-fall deposits, obsidian dike, Eburru Peak trachyte, obsidian lava flow, lava domes and pyroclastic cones, older Badland basalt, Cedar Hill lava dome, volcanic soil, and Eburru pumice-fall deposit.
3. The Eburru Geothermal Prospect consists mainly of Ol Doinyo Opor pumice-fall deposits which may be intruded by many dikes.
4. North-south trending faults develop in the prospect. Along the faults lava domes and

pumice cones of obsidian, scoria cones of basalt, fumaroles, and altered zones are formed.

5. Present surface is covered with two layers of pumice-fall deposits, Eburru-a pumice-fall deposits (younger) and Eburru-b (older), respectively.

6. It is uncertain whether the welded tuff and phonolite and comendite lava flow, which are exposed in the east of the survey area, distribute widely under the prospect or not.

7. Schematic profile of the prospect in E-W direction is shown in Fig. 3. It is very necessary to confirm the thickness of OI Doinyo Opor pumice-fall deposits and whether welded tuff and lava flow are extensively distributed under the prospect or not.



Fig. 3 Schematic Profile of The Eburru Geothermal Prospect in E-W Direction

Rock Alteration Survey

1. The rock alteration in the Eburru Geothermal Prospect can be divided into three zones and three distribution areas on the basis of mineral association.

2. The alteration zones give a zonal arrangement from zone I to zone III in the northern area of Eburru Crater.

3. Zones I, II and β - cristobalite area were formed under the condition of vapor-dominated geothermal system, and they are distributed in the Eburru Crater area extending E-W direction.

4. Zone III was found in the northern foot of the Eburru Crater area extending N-S direction, and calcareous sinter area was formed by hot-water which flows from the Eburru Crater area to the Eburru Station area along the water tables.

Geochemistry

In the course of field survey on the geochemical exploration, the Eburru Prospect was divided into three areas, the Northern, Central and Southern ones.

1. According to the results by geochemical exploration using carbon dioxide measurement in 1 meter depth soil air, it is supposed that two areas, the Eburru Crater area in the Southern area and the Central area, have high potential in geothermal resources within the whole survey area.
2. According to the results by 1 meter depth ground temperature measurement, however, the higher temperature areas have been found both in the Southern and the Northern area including the Eburru Station area.
3. The facts stated above lead us to the following assumption:
 - (a) In the Southern area, high geothermal potential area may exist, especially in the Eburru Crater area and in the area of about 500 meters south of Eburru Peak may have high geothermal potential.
 - (b) The geothermal potential in the Central area is higher than that in the Northern area, furthermore, the distance to the groundwater table from the surface of the ground in the Central area is larger compared with that in the Northern area.
4. The distribution trend of air contamination to the steam samples reported by UN gasgeochemical expert is also supporting the above stated assumption in 3-(b). Standing on the previous data reported by the same UN expert, we can make the same assumption that the steam samples from the shallow reservoirs in the Southern area (depth is less than several hundreds meters) contain CO₂ less than 0.4 volume percent. The quality of steam given by our assumption is adoptable for the ordinary usage for electric generation using turbine.

Geophysics

1. In the Eburru Crater area and in the Eburru Station area, generally the thick low resistivity layer with the resistivity of 10 ohm meters to 30 ohm meters underlies a series of thin high resistivity layers, total thickness of which is approximately 10 meters to 150 meters.

2. In the Eburru Crater area, we detected the higher resistivity layer under the thick low resistivity layer by several Schlumberger soundings. The depth to the top of the higher resistivity layer which we could detect by Schlumberger soundings of maximum current electrode spacing being less than 1500 meters is less than 1000 meters. However, we could not detect the bottom of the high resistivity layer by many Schlumberger soundings. Therefore, the resistivity of the higher resistive layer cannot be defined but it must be higher than 40 ohm meters.

3. The higher resistivity layer can be:

- (a) A basement crystalline rocks with high resistivity.
- (b) A steam filled geothermal reservoir with moderate resistivity.

4. By some Schlumberger soundings at the center of Eburru Crater, the above mentioned low resistivity layer is very thin and the high resistivity layer with resistivity of over 100 ohm meters underlies the low resistivity layer from the depth of 50 to 230 meters. The geological meaning of the appearance of the high resistivity layer in shallow place can be as follows:

- (a) Because of alteration, porosity of rock is decreased.
- (b) Steam filled pore instead of water.
- (c) Compact intrusive rocks intruded in the area.

5. In the Ceder West area, resistivity sequences change only very little horizontally. Under the surface layer, there is low resistivity layer with the resistivity of several tens of ohm meters. The resistivity of this low resistivity layer is lower at the center of the area and higher at the both side of the area. Topography of the Ceder West is like a valley and the center is at its bottom. Therefore, we assume the geothermal fluid flows from the Eburru Crater area to the Eburru Station area through the valley bottom of the Ceder West area.

6. In the Eburru Station area, we could not detect any high resistivity layer under the thick low resistivity layer. This fact may mean that the underground water table may be very shallow and the thickness of the water filled layer, with warm water, may be very thick, and the underlying high resistivity layer of steam-filled layer or basement crystalline rock is very deep, deeper than 1000 meters. However, the geological interpretation of the Schlumberger sounding data must be waited until further geological information of the area, especially by drilling, is obtained.

RECOMMENDATIONS

1. As a result of the survey, we recommend that shallow exploratory wells (depth to approx. 400 meters) are to be drilled at the following sites (see Fig. 4).

Site I : The rock alteration survey suggests that this site may be the center of heat source in the Eburru Geothermal Prospect and Schlumberger electrical soundings found that the high resistivity layer is very shallow (less than 100 meters). Both the concentrations of carbon dioxide and mercury in soil air are high and the ground temperature is also high.

Site II : This area has high concentration of carbon dioxide and high ground temperature and is supposed by the geochemists that the hot water table may be relatively deep. Geologically O1 Doinyo Opur pumice fall deposits, banded obsidian and the underlying rocks need to be studied by drilling at the site II.

Site III : The rock alteration study shows that the site III is the most active geothermal area in the Eburru Station area. Strong steam manifestation has been seen in the area and low grade anomalies in carbon dioxide concentration and in the ground temperature distribution have also been recognized. Geologically, the information, e.g. thickness and distribution of the banded obsidian and rocks underlying the banded obsidian are needed to be obtained.

Site IV : This site is in the different drainage area from Eburru Crater. The resistivity survey suggests a relatively high resistivity layer has been seen under the thick low resistivity layer at the site IV. The gravity map shows steep gravity gradient toward west of the site IV.

Site V : The strong geothermal manifestation is in the site V and relatively low but clear anomalies in carbon dioxide and in ground temperature are seen. The electrical resistivity survey suggests that relatively thin high resistivity layer (thickness is less than 100 meters) overlies the low resistivity layer, of which bottom has not been seen by our survey in the Eburru Station area.

Site VI : When drilling at the site II, the technical difficulties of transporting drilling rig and other material may be expected due to the topographical conditions of the location of the site II. Therefore we recommend the site VI as a substitute site for the site II.

2. When the shallow exploratory wells be drilled, it is necessary that rock core samples must be taken and temperature must be measured.
3. To obtain the reliable underground geoscientific and engineering data which lead to the evaluation of the geothermal potential in the Eburru Prospect, the drilling of the first deep exploratory well with the depth over 1,000 meters is recommended to be carried out after the shallow exploratory wells being drilled.
4. Gravity map of much broader area, from Naivasha Lake to Lake Elementeita and from Nakuru-Naivasha road to the west bank of the Rift Valley is necessary to study the macroscopic mechanism of the geothermal system.
5. Around the Soysambu farm, dipole mapping survey shows very low resistivity zone, which is needed to be studied in near future.
6. This survey shows that the geothermal area probably extends in the surrounding area. Therefore, we recommend that the similar survey is to be carried out in the surrounding area to make the extension of the geothermal area clear.

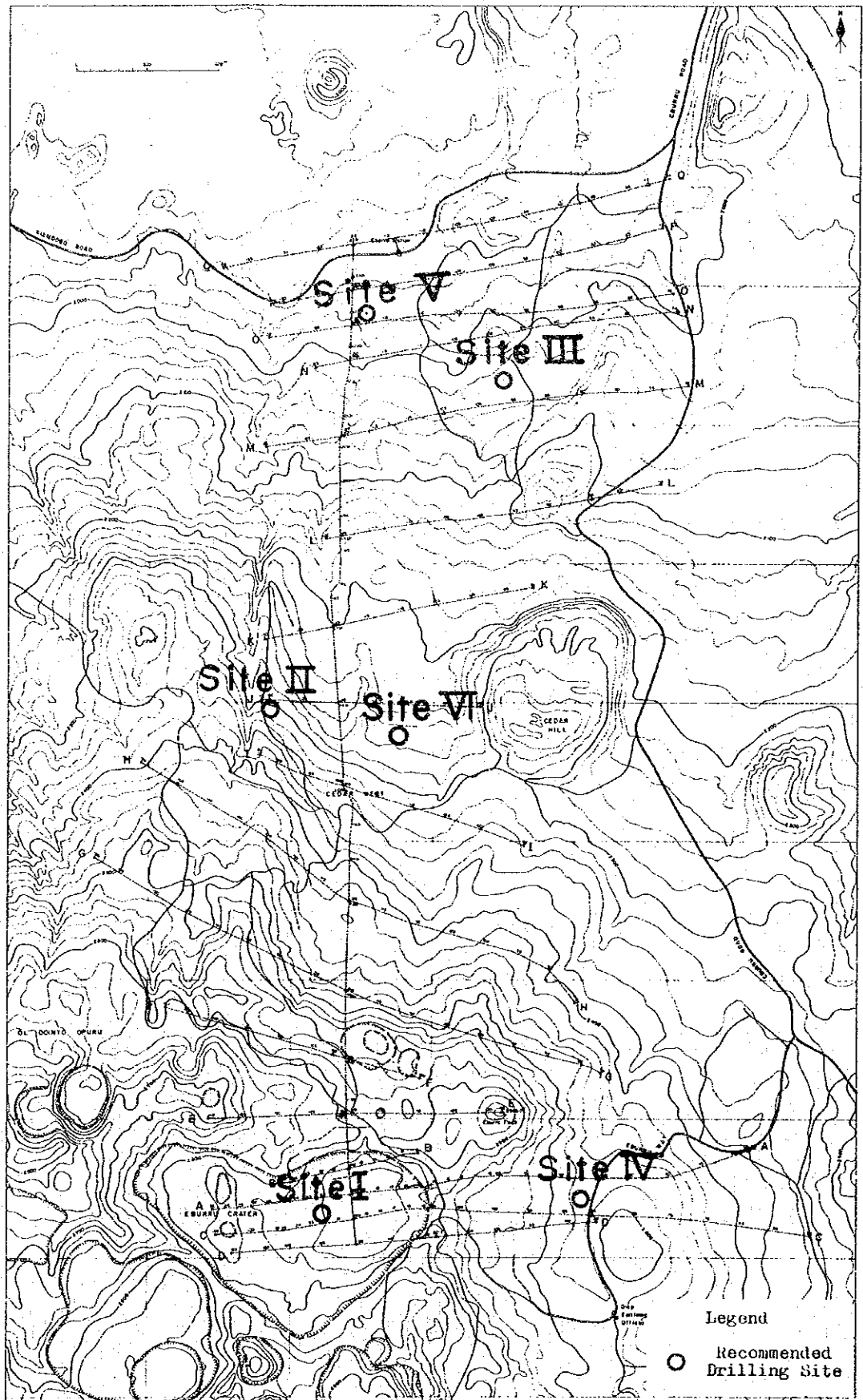
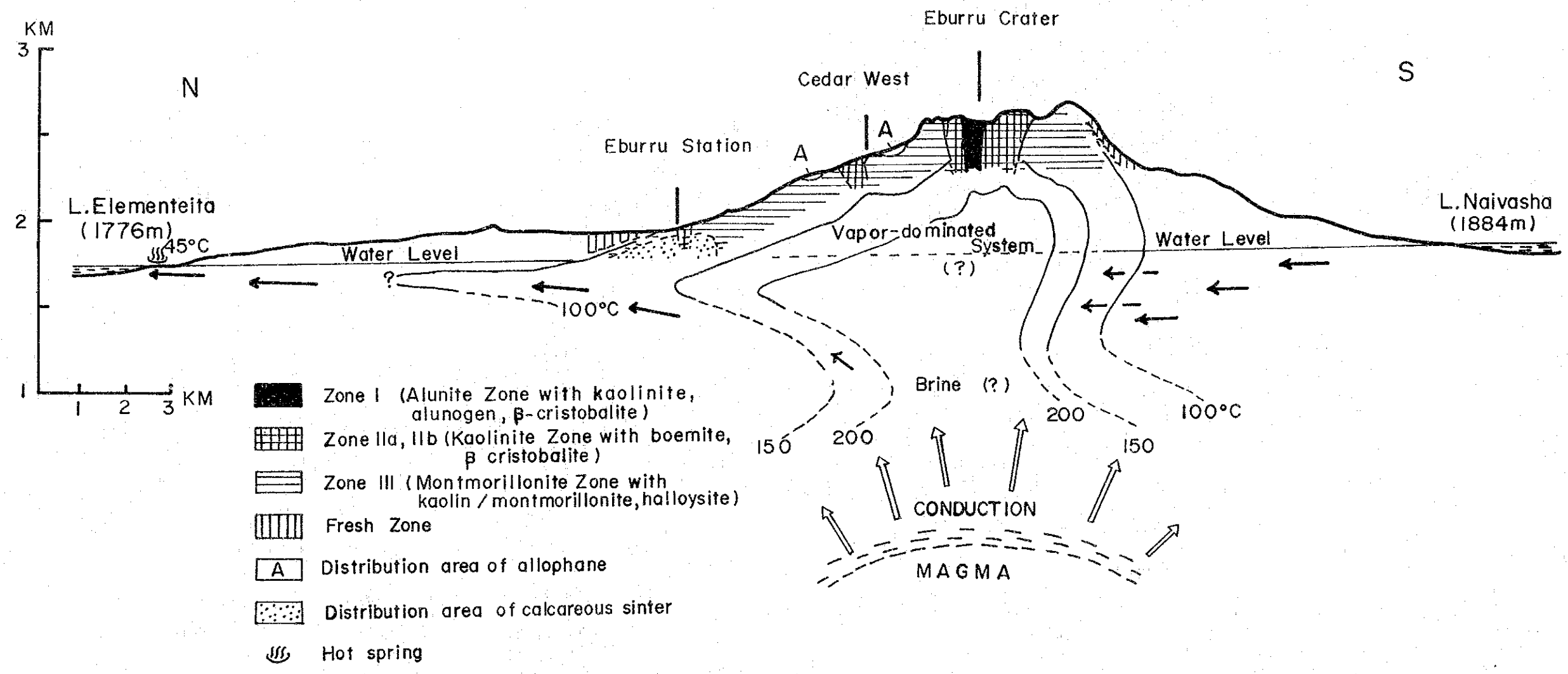


Fig. 4 Recommended Exploratory Drilling Sites

Fig. 5 Genetic Model of Eburru Geothermal Area



CONTENTS

PREFACE

LOCATION MAPS

CONCLUSIONS

RECOMMENDATIONS

I. OUTLINE

Chapter 1	Introduction	1
1.1	Purpose of the Project	1
1.2	Location and Extent of the Survey Area	1
1.3	The Survey	1
1.4	Team	2
1.5	Circumstances	3
Chapter 2	General Description of The Survey Area	5
2.1	Location	5
2.2	Topography	5
2.3	Valley	5
2.4	Fault	5
2.5	Geographical Naming	6

II. GEOLOGICAL SURVEY

Chapter 1	Introduction	9
Chapter 2	Summary of Geology	11
2.1	Geology	11
2.2	Fault	11
Chapter 3	Details of Geology	13
3.1	Basement	13
3.2	Eburru Volcano	16

III. GEOCHEMICAL SURVEY

Chapter 1	Introduction	27
Chapter 2	Survey Method	29
2.1	General Explanation	29

2.2	Setting of Survey Lines and Stations	29
2.3	Measurement	30
2.4	Mercury Measurement in Soil Air	30
2.5	Carbon Dioxide Measurement in Soil Air	33
2.6	1 Meter Depth Ground Temperature Measurement	34
2.7	Mercury Content Measurement in Soil	35
2.8	Relation of Repeated Measurement at the Same Point	35
Chapter 3	Results	37
3.1	General Explanation	37
3.2	1 Meter Depth Ground Temperature Measurement	37
3.3	Carbon Dioxide Content Measurement in Soil Air	38
3.4	Mercury Concentration in Soil Air	38
3.5	Mercury Concentration in Soil	39
Chapter 4	Discussion	41
4.1	1 Meter Depth Ground Temperature	41
4.2	Carbon Dioxide Content Measurement in Soil Air	41
4.3	Mercury Content Measurement in Soil Air	43
IV. GEOPHYSICS		
Chapter 1	Introduction	55
1.1	Relation Between Resistivity and Rocks	55
1.2	Electrical Survey in Eburru	56
Chapter 2	Field Work	57
2.1	Instruments	57
2.2	Field Procedure	57
2.3	Data Reduction	58
2.4	Interpretation of Data	59
Chapter 3	Results	61
Chapter 4	Interpretation	65
V. ROCK ALTERATION SURVEY		
Chapter 1	Introduction	99

Chapter 2	Geological Setting	101
Chapter 3	Outline of Geothermal Activities	103
Chapter 4	Specimens and Method of Study	105
Chapter 5	Alteration Products	107
Chapter 6	Zonal Distribution of Alteration Zones	109
Chapter 7	Discussion	111
	Supplement for Rock Alteration Survey in the Interim Report II (1981)	113

APPENDIX

1 X-Ray Diffraction Data for Altered Rocks

LIST OF FIGURES

- Fig. 1 and 2 Location of Project Area
- Fig. 3 Schematic Profile of the Eburru Geothermal Prospect in E-W Direction
- Fig. 4 Recommended Exploratory Drilling Sites
- Fig. 5 Genetic Model of Eburru Geothermal Area
- Fig. II-1 Locality Map of Thin Section Samples
- Fig. II-2 Geological Map of the Eburru Prospect
- Fig. II-3 Geological Sequences of the Eburru Geothermal Prospect
- Fig. II-4 Columnar Section of Ol Doinyo Opor Pumice-fall Deposits at Point-39
- Fig. II-5 Distribution of Eburru-a (upper) and Eburru-b (lower) Pumice-fall
Deposits (cm)
- Fig. II-6 Eburru Geothermal Prospect, Viewed from North
- Fig. II-7 Ol Doinyo Opor Pumice-fall Deposit at Point-291
- Fig. II-8 Flow Structure of Obsidian Dike at Point-208
- Fig. II-9 Flow Structure of Obsidian Dike at Point-208
- Fig. II-10 Obsidian Dike (D) Intruding to Pumice (P) at Point-175
- Fig. II-11 Eburru-a and -b Pumice-fall Deposits at Point-161
- Fig. III-1 Mercury Spectrometer
- Fig. III-2 Carbon Dioxide Detector
- Fig. III-3 Histogram of 1 Meter Depth Ground Temperature in the Eburru Prospect
- Fig. III-4 Histogram of Common Logarithm of CO₂ (%) in Soil Air in the Eburru
Prospect
- Fig. III-5 Histogram of Common Logarithm of Hg (ng/l) in Soil Air in the Eburru
Prospect
- Fig. III-6 Histogram of Common Logarithm of Hg (ppm) in Soil in the Eburru Prospect
- Fig. III-7 Histogram of 1 Meter Depth Ground Temperature in the Southern Area (line
A to E)
- Fig. III-8 Histogram of 1 Meter Depth Ground Temperature in the Central Area (line F
to K)
- Fig. III-9 Histogram of 1 Meter Depth Ground Temperature in the Northern Area (line
L to Q)
- Fig. III-10 Histogram of Common Logarithm of CO₂ in Soil Air in the Southern Area
(line A to E)

- Fig. III-11 Histogram of Common Logarithm of CO₂ in Soil Air in the Central Area (line F to K)
- Fig. III-12 Histogram of Common Logarithm of CO₂ in Soil Air in the Northern Area (line L to Q)
- Fig. IV-1 Schlumberger Electrode Configuration
- Fig. IV-2 Wiring of Equipment
- Fig. IV-3 Distribution of Apparent Resistivities (at AB/2=500m)
- Fig. IV-4 VES Curve and Computer Model
- Fig. IV-5 Apparent Resistivity Sections
- Fig. IV-6 Resistivity Sections

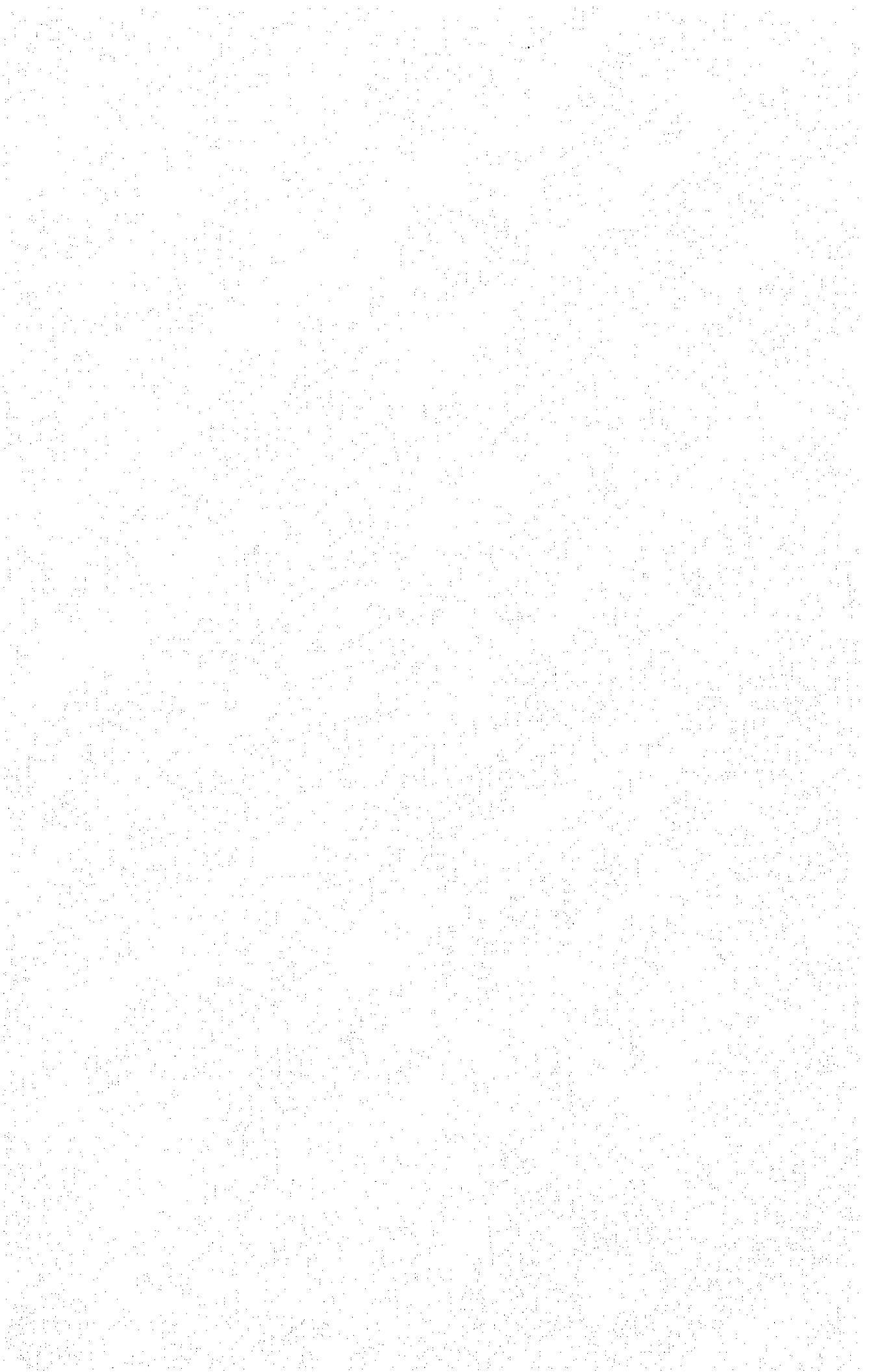
LIST OF TABLES

Table II-1	List of Thin Section Samples
Table III-1	Survey Lines and Stations for Geochemical Survey in the Eburru Prospect
Table III-2	Histogram of 1 Meter Depth Ground Temperature
Table III-3	Histogram of Common Logarithm of CO ₂ Value in % in Soil Air
Table III-4	Histogram of Common Logarithm of Hg (ng/l) in Soil Air
Table III-5	Histogram of Common Logarithm of Hg (ppm) in Soil
Table IV-1	Statistics of Apparent Resistivities at AB/2 = 500m
Table IV-2	Resistivity Field Data
Table V-1	X-ray Diffraction Data for Altered Rocks

LIST OF PLATES

Pl. III-1	Survey Lines and Stations
Pl. III-2	Distribution of 1 Meter Depth Ground Temperature
Pl. III-3	Distribution of Carbon Dioxide Content in Soil Air
Pl. III-4	Distribution of Mercury Content in Soil Air
Pl. III-5	Distribution of Mercury Content in Soil
Pl. III-6	Compiled Geochemical Anomalies
Pl. III-7	Lineament Map of the Prospect
Pl. V-1	Distribution Map of Hot Grounds Detected by IR Survey of the UNDP
Pl. V-2	Zonal Distribution Map of Alteration Zones

I. OUTLINE



CHAPTER 1 INTRODUCTION

1.1 Purpose of the Project

The purpose of the project is to locate underground geothermal reservoir and to evaluate geothermal potential in the Eburru Geothermal Prospect. This project is a part of the Rift Valley geothermal development project in Ministry of Energy, the Republic of Kenya.

In the course of executing the survey, survey technique and theoretical background of the survey were transferred to technical personnel of the Ministry.

1.2 Location and Extent of the Survey Area

The project area is centered by Eburru location, Naivasha division, Nakuru district, Rift Valley Province and is approximately 950 sq. km (see Fig. 1 and Fig. 2). The actual survey is mostly concentrated in the area of about 100 sq. km, 10 km wide in the east-west and 10 km long in the north-south.

1.3 The Survey

(i) Study of Publications and General Examination

Publications concerning the survey area were collected and studied to make the survey program and to prepare for the survey in the area.

(ii) Geological Survey

Geological mapping was carried out in the area of 100 sq. km.

Seventy thin sections of rock samples were studied under microscope.

Alteration of rocks was studied and distribution of altered mineral was mapped in the area of 45 sq. km. One hundred and sixty rock samples were collected and about one hundred samples were studied by X-ray diffractometer in Ministry of Energy and in Geological Survey of Japan.

(iii) Geochemical Survey

As geochemical survey the following are studied.

Hg concentration	1143 points
CO ₂ concentration	1142 points
Temperature in 1 meter deep	1143 points
Soil Sample	1163 pcs.
Condensed water sample	8 pcs.

The measurements were done mostly every 50 m along seventeen lines and in about 30 sq. km area.

(iv) Geophysical survey

Geoelectrical soundings by Schlumberger electrode array were carried out. The following are the specifications.

Total length of the survey lines	33.2 km
Number of the survey lines	12 lines
Number of measurements	81 pts.

1.4 Team

The member of the survey team are made up of Japanese and Kenyans and are follows:

Japanese

Koji Motojima* (Leader)
(Geochemist/Geologist)

Yoshiaki Sato* (Geologist)

Hiroyuki Satoh* (Geologist)

Kenzo Baba*
(Geologist/Geophysicist)

Jiro Komai* (Geophysicist)

Harukichi Shimode**
(Drilling Engineer)

Tadao Mizoguchi**
(Geochemist/Geophysicist)

Kazuo Hirowatari**
(Geochemist)

Takashi Ohya**
(Geophysicist)

Keiji Kimbara*
(Geologist)

Isao Sato*
(Geophysicist)

Kenyans

W.J. Wairegi
(Director of Technical Division)

J.K. Kinyariro (Co-Leader)
(Geochemist)

J. Barongo (Geophysicist)

D.K. Kilele
(Geophysicist Trainee)

C. Wanjie (Geochemist Trainee)

H.K. Andambi
(Geological Assistant)

F.N. Ibutu
(Geological Assistant)

D. Jacca L.
(Geological Assistant)

D. Kamau
(Geological Assistant)

J.M. Ndolo
(Geological Assistant)

P. Mwangi
(Geological Assistant Trainee)

Ryohei Ohtsubo**
(Geophysicist)

Setsuo Takemoto***
(Coordinator)

Keiichi Kato***
(Coordinator)

Kazuhiro Yoneda***
(Coordinator)

* Geological Survey of Japan

** Mitsui Mineral Development Engineering Co., formerly called MESCO Inc.

*** Japan International Cooperation Agency.

The JICA survey team was sent to Kenya four times during 1979 and 1982 and has worked in the field totally about four month. The itinerary of the JICA survey team is as follows:

	from	to
Scope of work mission	22 October, 1979	5 November, 1979
1st Phase Mission	3 December, 1979	10 March, 1980
2nd Phase Mission	28 July, 1980	15 February, 1981
3rd Phase Mission	22 January, 1982	28 March, 1982

1.5 Circumstances

In Kenya, some hydro-power, fuel wood and geothermal power are only utilized domestic energy resources. Hydrocarbon resource has not yet being found in the country. Development of new energy resource has been long waited because electricity consumption has been increasing very rapidly and amount of payment for oil in her foreign exchange became impossibly high.

UNDP (United Nations Development Program) carried out geothermal exploration project in the Rift Valley in six years from 1970 to 1976. The UNDP survey team recommended the following three geothermal development programs;

- (i) continue to drill production wells in Olkaria area and obtain enough steam to generate electricity
- (ii) drill slim holes in Olkaria area in order to evaluate geothermal reserves of the area and to decide locations of production wells, and
- (iii) do reconnaissance survey in the following three areas (total area: 45km x 10km) to obtain information about geothermal potential.

- (a) Kedong Valley: Area between Suswa Mountain and Hells Gate
- (b) Naivasha-Eburru: Area between Olidien Bey and Lake Elememteita
- (c) East Molo: Area between Menengai Crater and Lake Bogoria.

The government of Kenya ordered Mines and Geology Department of Ministry of Natural Resources to follow the UNDP recommendations. Mines and Geology Department requested the Japanese government to take up the recommendation (iii) and to survey geothermal areas in the Rift Valley.

The Japanese government sent the preliminary survey team to Kenya through the Japan International Cooperation Agency (JICA). Because of the creation of new Ministry of Energy in the Kenyan Governmental structure on November 1979. The geothermal exploration is now under the Ministry of Energy.

The survey area, Eburru area, neighbours the Olkaria geothermal area. Its geological environment is similar to that of the Olkaria area. Currently Olkaria generates 15 MW electricity and other 15 MW plant is under construction. Kenya became the first nation in African continent to produce electricity from geothermal steam.

CHAPTER 2 GENERAL DESCRIPTION OF THE SURVEY AREA

2.1 Location

The Eburru Geothermal Prospect is located about 16km to the north west of Lake Naivasha (altitude 1,890m) in the Rift Valley. The prospect area measures about 10 km from east to west and 10 km from north to south and in the center of the area. Eburru Peak (2,668m) rises.

2.2 Topography

The area around Eburru Peak, 2,500m to 2,600m in altitude, has been cultivated. Toward north and east the altitude decreases and finally reaches to 2,000m at the bottom of the Rift Valley.

To the west, however, altitude increases to 2,800m in Ol Doinyo Oporu forest region.

Configuration of the prospect is rather gentle, but it is broken up by Eburru Peak, lava domes, pyroclastic cones, and explosion craters. The diameters of the explosion craters vary from 100 m to 750 m and altered pumice is usually seen around them.

There is a large dipression, so-called "caldera", to the southwest of Eburru Peak. It measures 2 km from east to west and 1 km from north to south. The depression is not a caldera but a composit explosion crater.

2.3 Valley

Valleys in the prospect have no water except during a heavy rain. Trending of the valleys runs mostly south to north, possibly having the close relationship with the direction of the major fault system in the Rift Valley area. These valleys generally have narrow valley bottoms with deeply cut wall (20 m to 40 m deep). However, the direction of valleys around Eburru Peak, the lava domes, and the pyroclastic is variable subsequent to their prominent topography. The valleys have rather shallow and wide valley bottoms.

Around the altitude of 2,200m to 2,400m where rocks are composed of pumice fall deposits, the valleys disappear abruptly and above the point, where the valleys disappear, the land becomes flat.

2.4 Fault

Faults, extending north to south, develop in the Eburru Geothermal area. Most of them are clearly reflected on the topography of area. Details of the faults will be discussed in the Section

II "Geology".

2.5 Geographical Naming

In the topographic map (scale 1 to 50,000), published by Survey of Kenya, there are not many places in the survey area where names are given. In order to avoid difficulty of describing the area in this report, we named several places which are as follows:

Eburru Peak: the triangular point of which elevation is 2,668m.

Eburru Station: along the Route E446 to Kiambogo, where former Eburru railway station was.

Eburru Crater: the largest explosion crater in the area at the west of Eburru Peak and the diameter is approximately 2 km.

Cedar Hill: the lava dome on the west of the Eburru Road D322.

Cedar West: the small village about 1 km west of the Cedar Hill.

II. GEOLOGICAL SURVEY

[The page contains extremely faint and illegible text, likely due to low contrast or scanning quality. The text is arranged in several paragraphs, but the individual words and sentences cannot be discerned.]

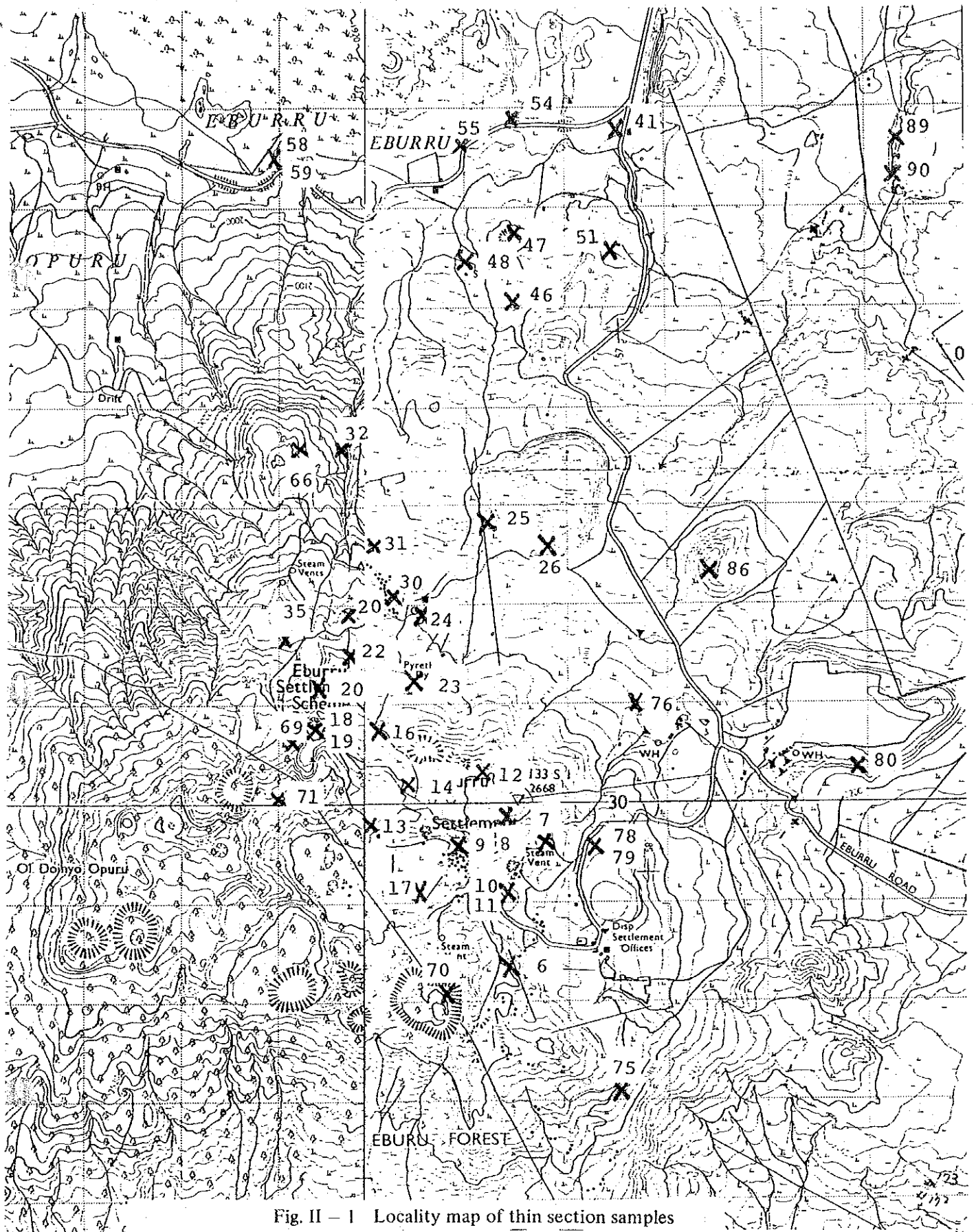
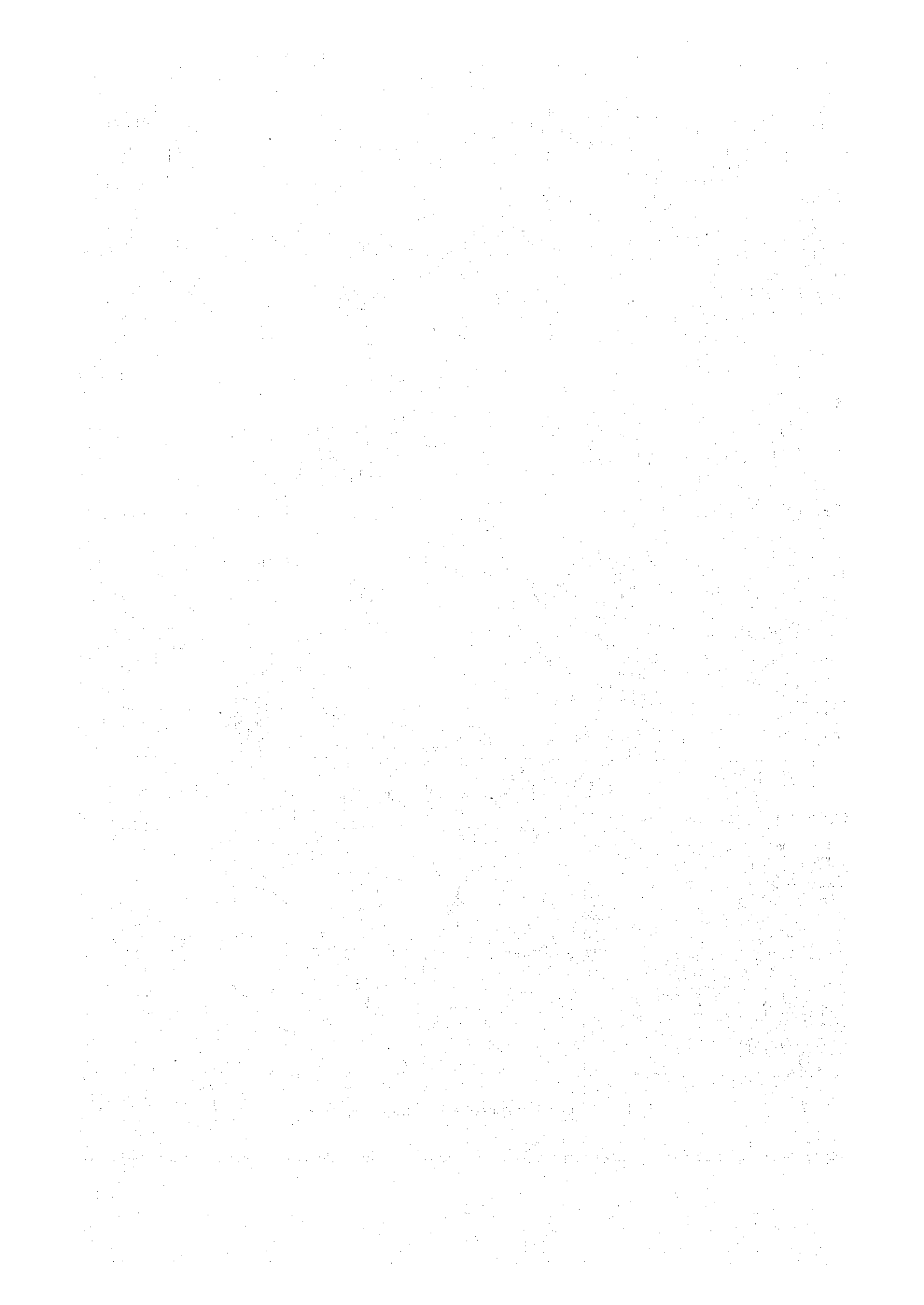


Fig. II - 1 Locality map of thin section samples





CHAPTER 1 INTRODUCTION

Geology of the Eburru Geothermal Prospect and its surroundings are surveyed with the topographic map on the scale of 1: 25,000 extended from the map on the scale of 1: 50,000 made by the Government of Kenya for the total number of 40 days.

Thin sections of rock samples were prepared by both the Mining and Geology Department, Ministry of Environment and Natural Resources, the Government of Kenya, and the Geological Survey of Japan, Agency of Industrial Science and Technology, MITI. Localities and list of the thin section samples are shown in Fig. II - 1 and Table II - 1, respectively.

CHAPTER 2 SUMMARY OF GEOLOGY

2.1 Geology

The rocks composed of the surveyed area are erupted and ejected volcanic rocks in the floor of the Rift Valley during Pleistocene and younger ages. Most of them are acid alkaline rocks. Pyroclastic fall deposits of same composition distribute extensively in the area, and there are no sedimentary rocks.

Welded tuff, exposed in the northeast of the surveyed area, may exist under the Eburru Geothermal Prospect and is considered to be the oldest rock in the area. The Prospect consists of pumice-fall deposits and obsidian dikes intruding them.

Two layers of pumice-fall deposits are recognized on the present surface. Thickness of the beds and grain size of pumices in it are decreasing toward west. Details of their distribution and craters erupting them, however, are not known clearly.

The nomenclature of acid alkaline volcanic rocks and identification of minerals described previously by some investigators are confused. A part of rock-forming minerals included in volcanic rocks are determined by means of the electron microprobe analysis. Phenocrysts are composed of sanidine (or : 31 ~ 42), arfvedsonite, aenigmatite (cosyrite) and sodium-rich ferrohedenbergite. Crystals in ground-mass are riebeckite, aegirin augite, aegirine and sanidine. Comendite includes quartz crystals both in phenocryst and ground-mass. Katophorite (Smith, 1931 ; Thompson and Dodson, 1963) is not yet identified. Geological map of Prospect is shown as Fig. II - 2.

2.2 Fault

North-south trending faults develop in the Eburru Geothermal Prospect. They were formed during Holocene age. Magnitude of fault movements was rather small-scale with little vertical throw. Extension of the faults can be traced about 5 km having 5 - 20 m throw. A fault striking N 15° E at eastern part of Kiambogo Road shows more than 50 m throw. Fault topography is clearly observed in the area.

Lava domes and pumice cones, scoria cone of basalt, fumaroles and altered zone are formed along the faults. On the other hand, we can estimate the presence of faults from the alignment of lava domes between Cedar Hill and Eburru Peak.

1. The first part of the document discusses the importance of maintaining accurate records of all transactions and activities. It emphasizes that proper record-keeping is essential for transparency and accountability, particularly in financial reporting and compliance with regulatory requirements. The text notes that incomplete or inconsistent records can lead to significant legal and financial consequences for the organization.

2. The second section addresses the role of internal controls in preventing fraud and errors. It highlights that a robust system of internal controls, including segregation of duties, authorization procedures, and regular audits, is critical for ensuring the integrity of the organization's financial statements. The document stresses that these controls should be designed to identify and prevent potential risks before they materialize.

3. The third part of the document focuses on the importance of communication and collaboration between different departments. It states that effective communication is necessary for the successful implementation of any initiative or project. The text encourages the use of clear, concise communication channels and the establishment of regular meetings to discuss progress and address any challenges that may arise.

4. The fourth section discusses the need for continuous improvement and learning. It notes that organizations should regularly evaluate their processes and procedures to identify areas for improvement. This can be achieved through the implementation of a quality management system, the use of key performance indicators (KPIs), and the promotion of a culture of learning and innovation. The document emphasizes that continuous improvement is essential for long-term success and competitiveness in a rapidly changing market.

5. The final part of the document provides a summary of the key points discussed and offers some practical recommendations for implementation. It reiterates the importance of accurate record-keeping, strong internal controls, effective communication, and a commitment to continuous improvement. The text concludes by stating that these principles are fundamental to the success of any organization and should be integrated into all aspects of its operations.

CHAPTER 3 DETAILS OF GEOLOGY

Summary of the succession of geology in the surveyed area is shown in Fig. II - 3.

3.1 Basement

3.1.1 Welded Tuff

The rock distributes narrowly in the northeast corner of surveyed area dipping 20° to the south with $N 70^{\circ} E$ strike. Similar rocks are underlying comendite (Thompson and Dodson, 1963) at northern side of Masai Gorge outside of the mapping area. The relation between the two welded tuffs is still unknown.

It is considered that the oldest known rocks in the Eburru Geothermal Prospect may be a kind of welded tuff. It is very important for further study to clarify the thickness and distribution of the welded tuff and related non-welded pyroclastic deposits under the Prospect.

3.1.2 Phonolite and Comendite Lava Flow

The rocks distribute to the east of the Eburru Road and are overlain by Ol Doinyo Opur Pumice-fall Deposits. Small-scale lava plateaus can be seen at south side of Masai Gorge and on the east of Eburru Road - Eburru Way intersection. Comendite which is cut by a fault is observed to the east of Eburru Road - Kianbogo Way intersection.

It is necessary for us to confirm phonolite or comendite lava flows under the Eburru Geothermal Prospect.

3.1.3 Ol Doinyo Opur Pumice-fall Deposits

The deposits distribute extensively in the Prospect and become thicker to west. They are intruded by many obsidian dikes (point - 175). They consist of accumulation of pumice-fall deposits, fine ashes and tuff breccias. Thickness of a single layer is usually about 3 meters (Fig. II - 4), however, above 20 meters at point - 175 (Fig. II - 10).

Pumices are angular and show a good sorting having a maximum diameter of 15 to 30 cm. These facts together with slight stratification show the characteristics of air-fall origin. Columnar section of the deposits at point - 39 is shown in Fig. II - 4.

Holocene	Eburru Volcano	Eburru-a Pumice-fall Deposit		obsidian faulting
		Eburru-b Pumice-fall Deposit		
		Volcanic soil		
		Cedar Hill Lava Dome	Ci	
		Older Badland Basalt	Bb	
Pleistocene	Basement	Lava dome and cone	Ld	
		Obsidian lava flow	Oi	
		Eburru Peak Trachyte	Et	
		Obsidian dike	!	
		Oi Doinyo Opur Pumice-fall Deposits		
		Phonolite and comendite lava flow	Vt	
		Welded tuff	Wt	

Fig. II – 3 Geological Sequences of the Eburru Geothermal Prospect

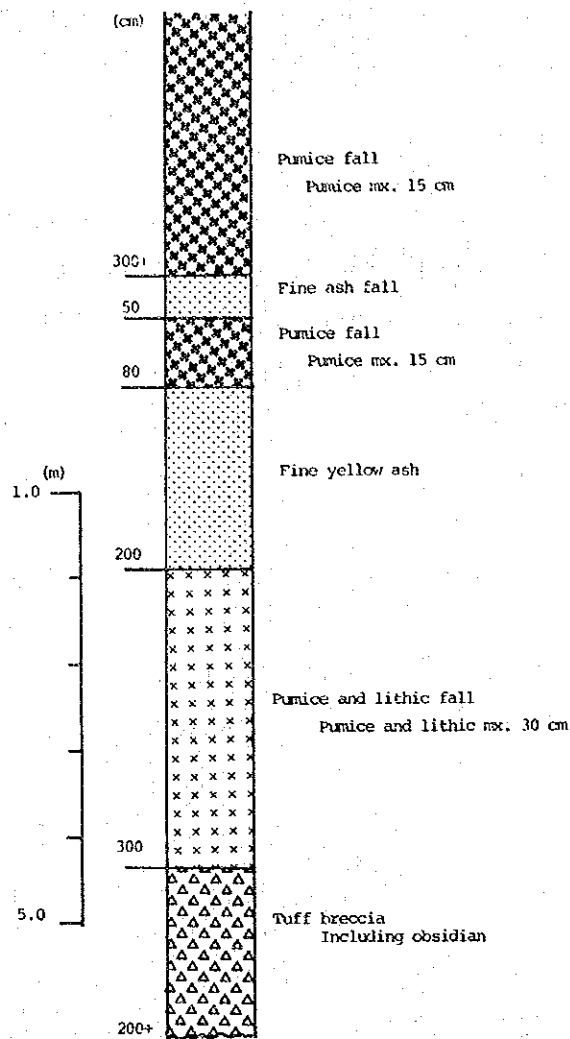


Fig. II - 4 Columnar Section of Ol Dolnyo Opur Pumice-fall
Deposits at Point 39

The distribution of the deposits extends further east of the Prospect, i.e. at the junction of Eburru and Kiambogo Road, hills west of the rail way and south of Masai Gorge. The deposits overly the phonolite and comendite lava flows.

Thickness of the deposits is estimated as about 2 to 3 hundreds meters on the Prospect. We expect that it will be confirmed as soon as possibly by shallow drillings.

3.1.4 Obsidian Dikes

The rocks also are scattered on the ground of the Prospect. They have well developed flow structure shown by glass flow, and alignment of bubbles and/or feldspar phenocrysts. Ptygmatic folding structures are seen in several points. Sometimes banding composed of black glass and

pale green material, 3 to 5 cm in wide, are observed. Trending of the flow structure is usually north-south direction, but some shows N 50° E or W and E-W in rare case, with dipping angle of 40 to 90°.

The occurrence of the rocks is not clear because they occur as isolated exposure. However, at point – 175 (Fig. II – 10), the obsidian intrudes vertically into the flat-lying pumice-fall deposits of 20 m (+) in thickness with N 40° W in strike. Chilled margin of 4 cm in thickness is formed. The rock is pale green inside and black glass at chilled margin. Accordingly, it seems that obsidians in the Eburru Geothermal Prospect are dike rocks intruding into the Ol Doinyo Opur Pumice-fall Deposits and trend of the flow structure shows direction of dike rocks.

3.1.5 Eburru Peak Trachyte

Eburru Peak are composed of this rock. Thompson and Dodson (1963) called the rock rhyolite. The rock is extruded along a north-south trending weak line connecting Cedar Hill and Eburru Peak. On the southern side a thermal altered zone are observed. The rock is not covered by Ol Doinyo Opur Pumice-fall Deposits.

3.1.6 Obsidian Lava Flow

The lava flow covers Ol Doinyo Opur Pumice-fall Deposits in the west of the Eburru Geothermal Prospect (point – 81) and a part of the flow reaches to Kiambogo Road. On the contrary to obsidian dikes, the lava has horizontal flow structure. At and near the base of a flow brecciation has developed, but the rock becomes massive and compact upwards.

3.2 Eburru Volcano

3.2.1 Lava Domes and Pyroclastic Cones

There are two lava domes, one to the northeast and the other to the east of Cedar Hill. Two north-south trending faults run through the latter dome. Pyroclastic cones are found, two in the southeast of the surveyed area, and one in the center. They are composed of dark gray ash, pumice and obsidian fragments.

3.2.2 Older Badland Basalt

The rock is olivine basalt and is distributed in the Eburru Station area. It has undergone thermal alteration. The portion of outflow of lava may be a scoria cone in the north of the area.

3.2.3 Cedar Hill Lava Dome

Cedar Hill is a large obsidian lava dome having a diameter of about 1.3 km at the bottom. Well preserved grooves resulted from the movement of the lava flow can be seen on the surface of the dome. The rock consists of partly compact black glass and partly many feldspar crystals.

3.2.4 Volcanic Soil

Fine-grained, reddish brown volcanic soil is distributed mostly in the Eburru Geothermal Prospect.

3.2.5 Eburru Pumice-fall Deposits

The present surface of the Eburru Geothermal Prospect is covered by the deposits. Two layers, older and younger ones, are recognized. The older one is named here Eburru-b Pumice-fall Deposits and the younger one Eburru-a Pumice-Fall Deposits. Thickness of each decreases toward east or to Masai Gorge. The center of the eruption may be one of those explosion craters in Ol Doinyo Opor. Their thickness is shown in Fig. II – 5.

Supplement

Minerals and their composition in the main volcanic rocks are shown below.

Petrography of volcanic rocks in the Eburru Geothermal Project

Eburru Pumice-fall Deposits

Alkali feldspar Or 40–42
Quartz
Arfvedsonite
Aenigmatite

Obsidian dike

Alkali feldspar Or 40–42
Aegirine augite → Aegirine Fe+Mn/Fe+Mn+Ca+Mg 62 → 91
Arfvedsonite
Aenigmatite

Comendite

Alkali feldspar Or 35–36
Aegirine augite → Aegirine Fe+Mn/Fe+Mn+Ca+Mg 52 → 93
Arfvedsonite
Anifmatite
Alkali amphibole (?)

Kenite (which is Olivine-bearing comendite, from Gilgil Quarry)

Alkali feldspar

Or 31–38 → 33–42

Quartz

Olivine

Fa 96 → 99

Hedenbergite → Aegirine augite

$\text{Ca}_{45}\text{Mg}_{3.5}\text{Fe}_{51.5}$ →

$\text{Fe}+\text{Mn}/\text{Fe}+\text{Mn}+\text{Ca}+\text{Mg}$ 58

Arfvedsonite (rare)

Aenigmatite (rare)

Ilmenite (rare)

→ from phonocryst to ground mass

REFERENCES

- NAYLOR, W.I. (1971–1972) : 1:25,000 Geologic map of the Eburru Area (unpublished).
- NOBLE, John W. and OJIAMBO, Sebastian B. (1975) : Geothermal exploration in Kenya.
- RICHARD, J.J. and NEUMANN van PADANG, M. (1957) : Catalogue of active volcanoes of the world including solfataral field. part IV, Africa and the Red Sea. 118p.
- SMITH, W.C. (1931) : A classification of some rhyolites, trachytes, and phonolites from part of Kenya Colony, with a note on some associated basaltic rocks. *Quat. Jour. Geol. Soc. London*, vol. LXXXVII, p. 212–258.
- THOMPSON, A.O. and DODSON, R.G. (1963) : Geology of the Naivasha Area. Rep. no. 55, Geological Survey of Kenya, 80p.

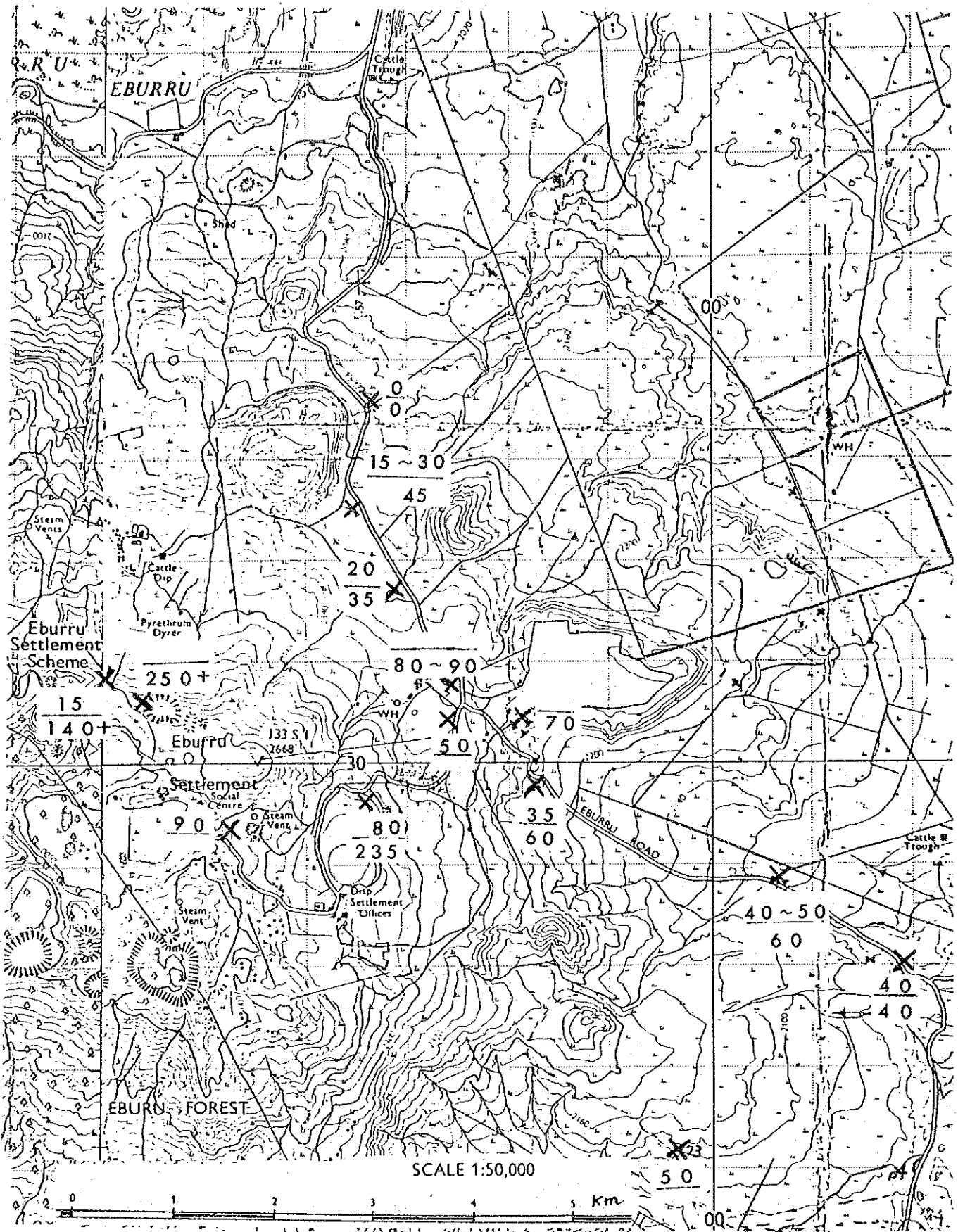


Fig. II - 5 Distribution of Eburru-a (upper) and Eburru-b (lower)
Pumice-fall Deposits (cm)

Table II - 1 List of thin section samples

K - 6	Gray blue. Floating rock at kaoline mine south of Eburru Primary School.
7	Black altered. Eburru Peak Trachyte.
8	Tufaceous green rock. Eburru Peak Trachyte.
9	Obsidian.
10	Pumice. Eburru-a.
10'	- do - (crushed)
11	Pumice. Overlain by K-10 (Eburru-a).
11'	- do - (crushed)
12	Gray rock. Eburru Peak Trachyte.
13	Altered rock at Kaoline mine in north wall of "caldera"
14	Altered rock, gray.
16	Pumice. Eburru-b.
16'	- do - (crushed).
17	Obsidian. Dike.
18	Pumice. Eburru-a.
18'	- do - (crushed).
19	Pumice. Eburru-b.
19'	- do - (crushed).
20	Rhyolite included in Pumice-fall deposits.
22	Pumice. Pumice-fall deposits.
23	Obsidian. Lava dome.
24	Pumice. Cinder cone.
24'	- do - Crushed.
25	Obsidian. Ceder Hill.
26	Green compact rock. Lava flow.
30	Obsidian. Flow-structured dike.
31	Welded tuff.
32	Obsidian. Lava.
35	Obsidian. Lava.
41	Comendite. Flow-structured.
42	Basalt. Badland Basalt. South of Lake Elementeita.
46	Green. Flow-structure. Lava flow.

- 47 Green comendite. Flow structure.
- 48 Scoria. Older Badland Basalt.
- 51 Floating rock. Comendite.
- 52 South Masai Gorge. Lava flow.
- 53 North of Masai Gorge. Lava flow.
- 54 Green compact Olivine-augite basalt. Older Badland.
- 55 Olivine-augite basalt. Older Badland Basalt.
- 58 Compact part.
- 59 Flow-structure.
- 66 Obsidian. Lava.
- 69 Comendite.
- 70 Pumice. Ejected from crater.
- 71' Pumice. Ejected from crater.
- 75 Obsidian. Flow structured. Dike.
- 76 Obsidian. Flow structured. Dike.
- 78 Pumice. Eburru-a.
- 79 Pumice. Eburru-b, overlain by K--78.
- 80 Green. Lava flow.
- 83 Green. East of K--83.
- 85 Olivine-bearing comendite. Flow structure, at quarry south of Gilgil.
- 86 Vesicular. Cone.
- 89 Flow structure.
- 90 Welded tuff.
- 95 Welded tuff. east of Naivasha.

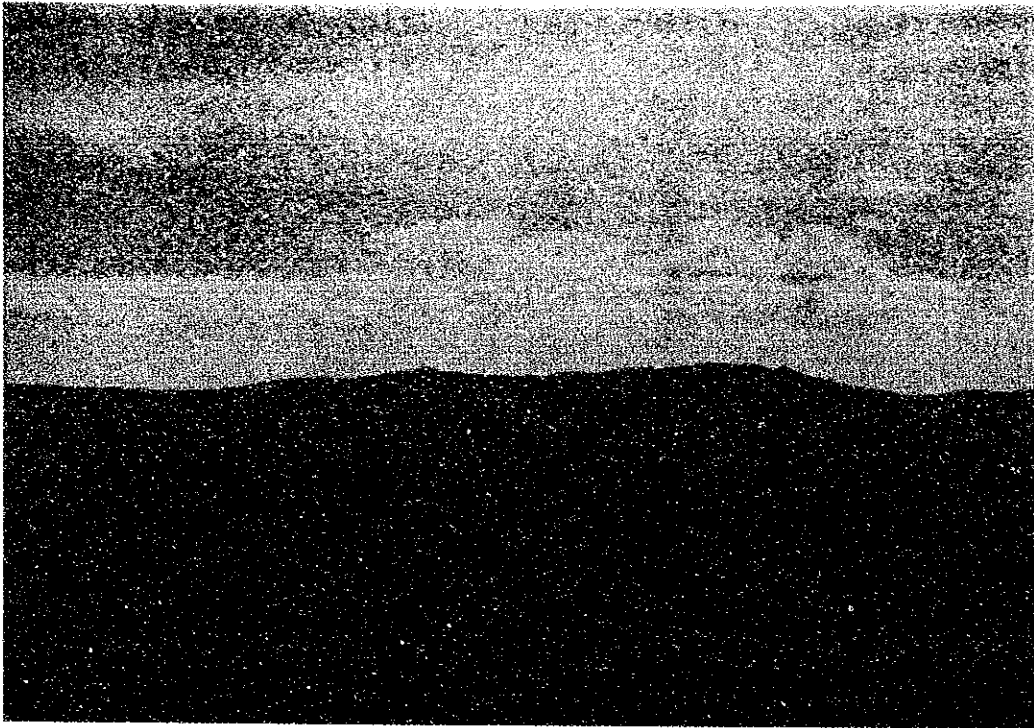


Fig. II - 6 Eburru Geothermal Prospect, Viewed from North.

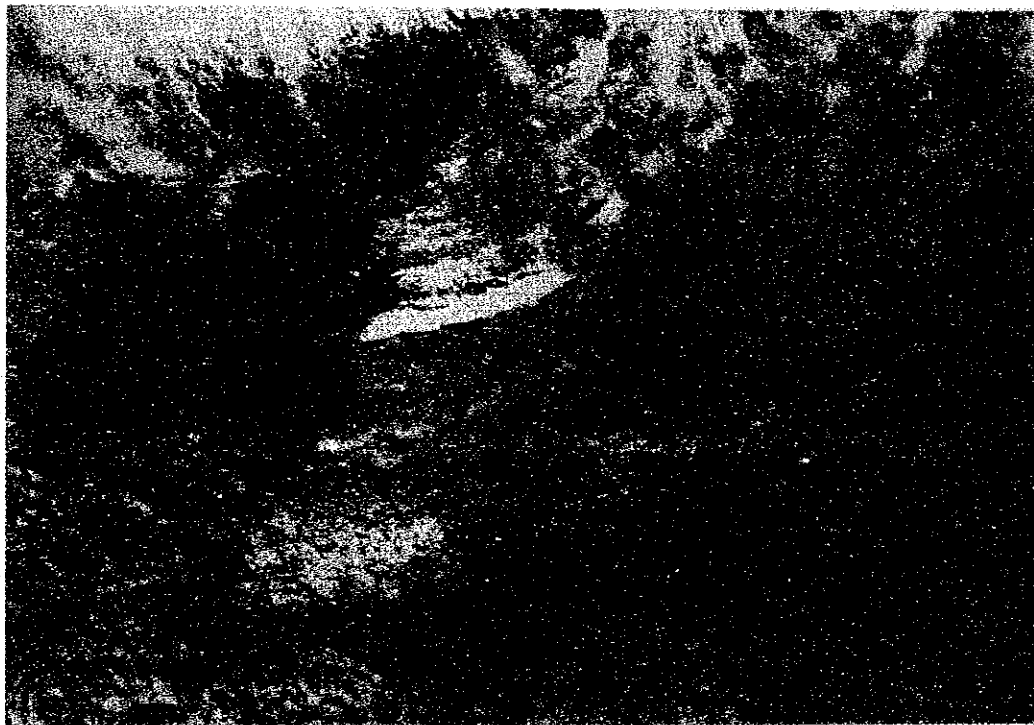


Fig. II - 7 Ol Doinyo Opur Pumice-fall Deposits at Point -291

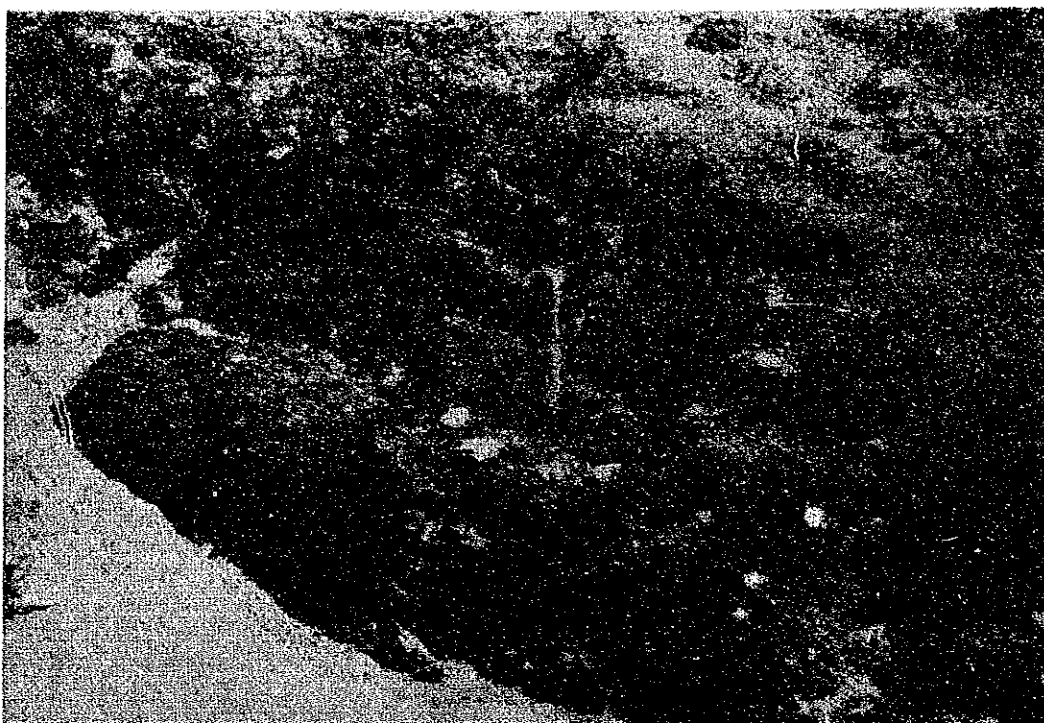


Fig. II - 8 Flow Structure of Obsidian Dike at Point -208.



Fig. II - 9 Ditto.



Fig. II - 10 Obsidian Dike (D) Intruding to
Pumice-fall Deposits (P) at Point -175.



Fig. II - 11 Eburru-a and -b Pumice-fall Deposits at Point -161.

III . GEOCHEMICAL SURVEY

CHAPTER 1 INTRODUCTION

In accordance with the general geochemical knowledge, the geochemical behavior of carbon dioxide in the igneous environment is relatively clear. The carbon dioxide of igneous origin is distributed in the igneous areas and controlled by the igneous activities not only in large scale but also in small scale. Therefore, the general distribution trend of carbon dioxide in soil air from 1 meter deep from the landsurface shows the general trend of the high temperature fluid reservoirs in relatively shallow depth (shallower than several hundred meters).

In addition to this, small scale distributional pattern of carbon dioxide in soil air, sometimes, indicates the existence of faults and if the geologic environment is very favourable, even the inclination (dip) of the fault can be determined by carbon dioxide distribution. The carbon dioxide concentration measurement using soil air has been adopted successfully by the JICA Mission since the beginning of field survey in February, 1980 in the Eburru Prospect.

The distribution of ground temperature at one meter deep from the landsurface has shown the good coincidence with the geothermal resources at various geothermal fields in the world. Therefore, the distributional data of shallow ground temperature should be prepared in the Eburru Prospect, and the JICA Mission has adopted this work since the beginning of field survey in early 1980.

The Rift Valley in Kenya is situated on one of the world's largest tectonic lines and has continuous movement with deep fault since late Miocene.

According to the global tectonics, the geothermal areas which are situated in the border regions between the two plates have some geochemical characteristics, for example high concentration in mercury and helium content. The bottom sea sediments along the East Pacific Rise have high value in mercury content and the bottom ocean water on the Rise has high helium content. The western region of USA is famous for its high concentration of mercury and potential geothermal fields. The fact shows that the geological phenomena of the deeper parts of the earth have a close relationship to the distribution of mercury and helium.

Standing on the basis stated above, the JICA Mission has successfully adopted the geochemical exploration method using mercury since the beginning of the field survey in the Eburru Prospect in early 1980.

Clear and reasonable coincidence has been recognized among the data on the shallow ground temperature, carbon dioxide in soil air, mercury in soil air and mercury in soil.

In the Eburru Prospect, no hot spring water from the surface of the ground has been reported and the gas-geochemical method should be applied in the area.

CHAPTER 2 SURVEY METHOD

2.1 General Explanation

Many large and small faults with north-south direction have been recognized and reported in the previous papers in the Eburru Prospect. Thus, the survey lines were arranged nearly east-west direction across the general geological trend.

According to the results of the first phase survey, early 1980, in the southern part of the Eburru Prospect, the east-west interval of survey points is preferably less than 50 meters, and the north-south interval of survey lines is preferably less than 300 meters. However, within the limited field survey period the whole area of the Eburru Prospect must be covered by the geochemical method, and at the initial stage of the field survey, it was decided that the east-west interval was 50 meters and the north-south interval was as close as the survey team could make.

2.2 Setting of Survey Lines and Stations

Before deciding the location of the survey lines and stations, we examined the following points:

- Prediction of weather condition during the field survey period.
- Manpower which we can use in the Eburru Prospect.
- Topographic condition.
- Vegetation condition.
- Condition of wild animals.
- Duration of field survey.
- Transportation condition.
- Supply of daily necessity.
- Condition of camp.

Finally, the survey lines and stations were decided as shown in Pl. III-1. The stone marker of triangulation on the top of Eburru Peak with the elevation of 2,668 meters above sea level was used as the topographic base station for the survey to the whole area of the Eburru Prospect.

The base line with general direction of north-south for the survey was set in the approximately central part of the area and 16 survey lines, on which many survey stations, having horizontal interval of every 50 meters, were arranged approximately perpendicular (east-west direction) to the base line. The direction of survey lines was determined by a magnetic compass, being called Ushikata Pocket Compass, with the approximate scale reading (sensitivity) of the 1/3 degree, and the distance was determined by a glass fiber tape measure.

Total numbers of survey stations and lines are 842 and 16 respectively, and the total length of the lines reaches 42.3 km in an area of 30 sq km (8 km in north-south and 5 km in east-west direction).

2.3 Measurement

Survey was carried out at each station as follows:

- (i) Two one meter deep holes are dug at each station.
- (ii) One of the two holes is used to measure carbon dioxide content in soil air three minutes after dug.
- (iii) The other hole is used to measure mercury content in soil air three minutes after dug.
- (iv) After the above mentioned measurements, one of the holes is used to measure 1 meter depth ground temperature.
- (v) Soil sample is collected at the bottom of 1 meter depth hole and is used for mercury content measurement. In the case of very dry hole, a surface soil sample is collected instead of 1 meter deep soil.

2.4 Mercury Measurement in Soil Air

For the current survey, the Scintrex mercury analyzer HGG-3 is employed because of its speed of analysis and its capability of insitu analysis.

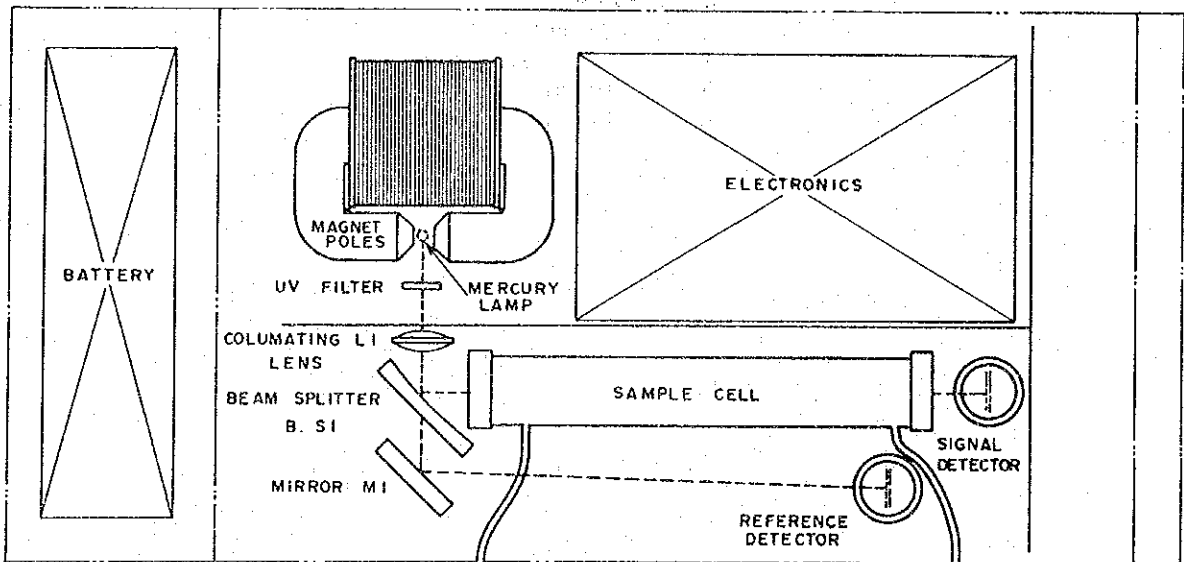
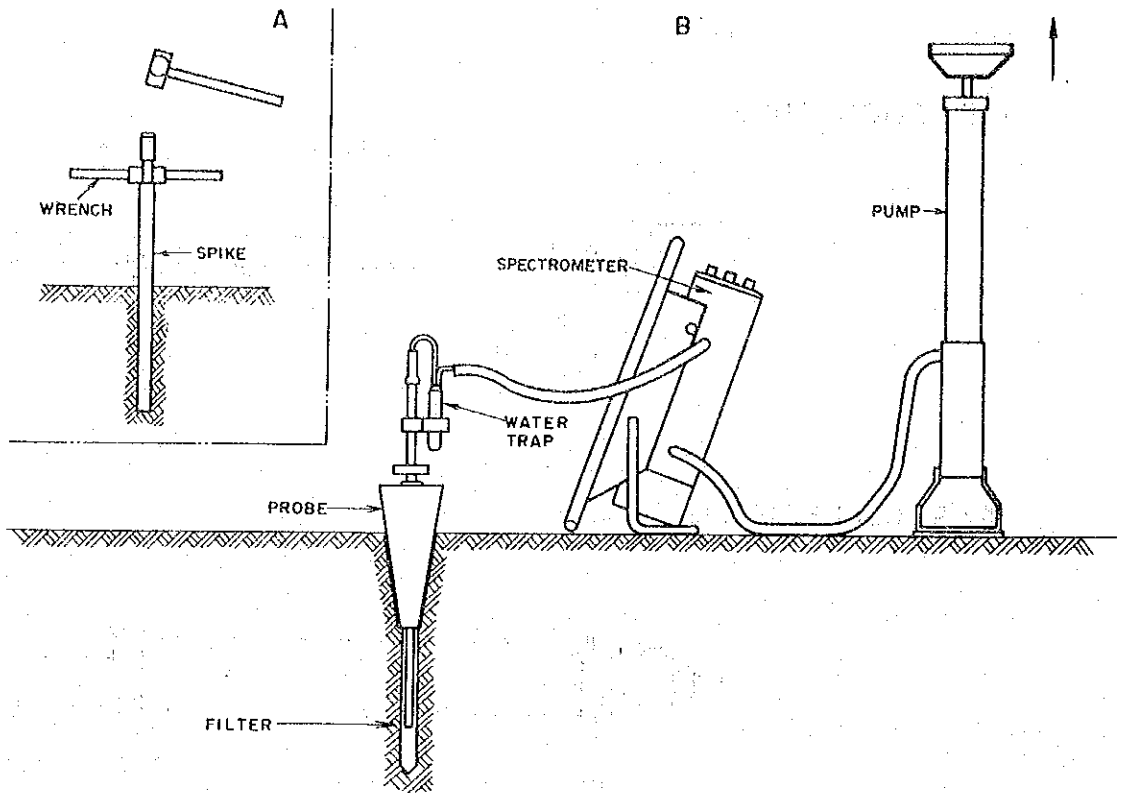
2.4.1 Equipment

The specifications of mercury spectrometer are as follows:

Manufacturer:	Scintrex Ltd.
Model:	HGG-3
Sensitivity:	better than 40 pg / 250 ml (0.16 ng / l)
Power:	lead dioxide – silica gel type batteries, 6 volts 6 ampere hour

The principle of the equipment is based on atomic absorption. The measurement is primarily the degree of attenuation by mercury vapor of the intense Hg emission line at 254 nm from a mercury lamp. There are, however, other common gasses and vapors which absorb ultraviolet strongly over wide wavelength range. The HGG-3 spectrometer employs a Zeeman Effect technique to generate a reference wavelength outside of the absorption envelop of the mercury spectrometer. By repetitively tuning on and off and strong magnetic field encompassing the mercury lamp, its emission is rapidly alternated from 254 nm to the reference wavelength. The

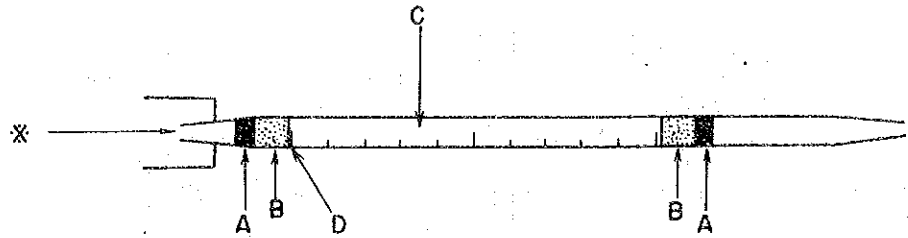
Fig. III - I MERCURY SPECTROMETER
SCINTREX HGG - 3



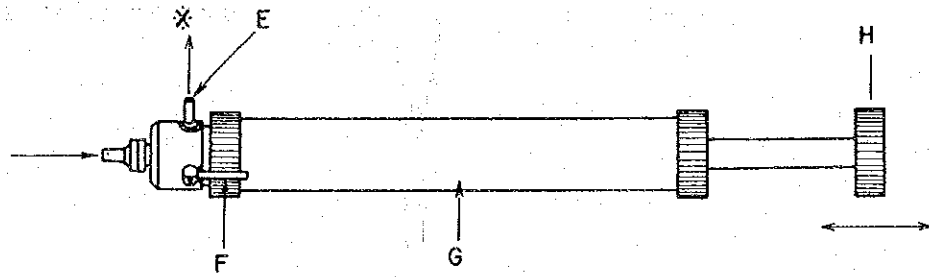
HGG-3 BACKPACK SPECTROMETER

Fig. III -2 Carbon Dioxide Detector

DETECTION TUBE



GAS COLLECTOR



- A stopper
- B glass grains
- C detection reagent (silicagel)
- D scale
- E tube connector
- F three ways valve
- G cylinder
- H piston nob

electronics then compare the absorption at the two wavelength and yield a measurement which is highly specific and highly sensitive for mercury.

2.4.2 Calibration

For calibrating the mercury analyzer, standard air sample of several specific mercury concentrations were made by diluting mercury vapor with an atmospheric air. As a result, mercury concentration and readings of the mercury analyzer in millivolt showed relatively proportional relation. Calibration was made repeatedly and all the calibrations relatively coincide each other.

2.4.3 Field Procedure

Procedure for the current field survey is as follows:

- (i) The equipment is warmed up.
- (ii) A stake with a diameter of about 20 mm is driven one meter into the ground.
- (iii) Immediately after the stake being pulled out, the probe with a plastic cone is forced into the opening until a good seal can be expected.
- (iv) Following the procedures stated on the operating manual of the mercury spectrometer, the maximum reading on the meter in millivolt is recorded.

While moving to the following station, the heater of the analyzer is kept on to keep it warm.

2.5 Carbon Dioxide Measurement in Soil Air

2.5.1 Equipment

Carbon dioxide gas detector (Fig. III-2) is used for measurement. Its specifications are as follows:

Manufacturer:	Komei Rikagaku Co.
Model:	Kitagawa detection tube, hand pump type ST and S
Range:	1 to 10 % and 1 to 20 %
Sample Volume:	50 ml
Pumping Time:	30 sec, 50 sec
Reagent in Tube:	Silica gel with special reagent.

The detection tube is very small and light, so it is very easy to carry in the field. Reading of carbon dioxide is only to measure the length of the part of the reagent where its color is changed against the scale printed on the detection tube.

2.5.2 Influence of Obstructive Gases

Over 1,000 ppm of nitrogen dioxide, over 3,000 ppm of sulfur dioxide, or over 3,000 ppm of hydrogen sulfide give the same coloring as carbon dioxide on the detection reagent, so that, without knowing non-existence of those obstructive gases, it cannot tell whether carbon dioxide or other obstructive gases exist in the air.

For the current survey, we measured sulfur dioxide concentration and hydrogen sulfide concentration in soil air at the points P-105, L-107, L-80, and near the point A-18. Sulfur dioxide was not detected at any point and hydrogen sulfide was not detected except at the point near A-18 where its concentration was 10 ppm.

Nitrogen dioxide content is not measured because it is hardly seen in geothermal area.

2.5.3 Field Procedure

Field procedure is as follows:

- (i) A stake with a diameter of 20 mm is driven one meter into the ground.
- (ii) Immediately after the stake being pulled out, a plastic tube with a rubber plug is inserted into the hole and forced a rubber plug into the opening of the hole until a good seal can be expected.
- (iii) Three minutes later, the detector pump is connected to the plastic tube. At first, air left in the plastic tube is removed by pumping so that only soil air is to be pumped into a detection tube.
- (iv) The piston of the detection pump is pulled to collect 50 ml of soil air from the ground.
- (v) Collected soil air is pumped into a detection tube, and color of detection reagent changes from pink to yellow.
- (vi) The ratio of the length of yellow part to that of unchanged reagent filled in the detection tube shows the concentration of carbon dioxide in soil air, and volume percent of carbon dioxide content is easily determined.

2.6. 1 Meter Depth Ground Temperature Measurement

2.6.1 Equipment

The specifications of the thermistor used is as follows:

Manufacturer: Takara Thermistor Instruments Co., Ltd.
Model: SPD-10
Sensitivity: 1 % of full scale

Range: Low: -5 degree C to 55 degree C
 High: 50 degree C to 110 degree C
Power: 1.5 v D-cell battery

2.6.2 Influence of Atmospheric Temperature Variation

It is important to study how deep in the ground diurnal temperature variation affects. The beginning of the survey on 30 January, 1980, temperature at 33 cm deep, 60 cm deep, and 93 cm deep in the ground was continuously recorded. Temperature variation at 93 cm deep in the ground between 8 a.m. and 7 p.m. was only 0.6 degree C while it at the surface of the ground was 11.5 degree C. Temperature variation curve at 93 cm deep does not show significant diurnal change. Even temperature at 33 cm deep in the ground did not show any significant change. Standing on the results, temperature measurement at 1 meter deep may have good response of the thermal condition in the relatively shallow place. (The result of the temperature measurements are shown on "Interim Report, 1980".)

2.6.3 Field Procedure

In the field, the following procedure is taken to measure 1 meter depth ground temperature.

- (i) The thermistor sensor is lowered into one of two 1 meter depth holes dug for soil air analysis.
- (ii) The sensor is left three to five minutes in the ground to obtain stable readings on the thermistor meter.

2.7 Mercury Content Measurement in Soil

In order to assure validity of mercury content in soil air and to know the accumulated mercury in the area, mercury content in 1 meter depth soil or surface soil was analyzed. When the soil is too dry to collect sample by a screw type auger, a soil sample is collected from the land surface instead of 1 meter deep in the ground. Collected samples were analyzed at the chemical laboratory of Mines and Geology Department in Kenya and the Central Laboratory of Mitsui Mining and Smelting Co., Ltd..

2.8 Relation of Repeated Measurement at the Same Point

At many survey points we repeated carbon dioxide measurement and 1 meter depth temperature on 1982. We studied variance of data and calculated regression equations which relate measurement on 1980 and it on 1982. The regression equation for carbon dioxide content

in soil air is :

$$\text{CO}_2 (80) = 0.14157 + 1.44262 \times \text{CO}_2 (82)$$

The regression equation for 1 meter depth temperature is :

$$\text{Temp} (80) = 1.58546 + 0.93629 \times \text{temp} (82)$$

where

CO₂ (80), Temp (80): measurement on 1980

CO₂ (82), Temp (82): measurement on 1982

All the data were calibrated into the data on 1980. For survey points which have two or more measurements, we calibrated 1982 measurements into 1980 measurements and calculated algebraic mean values and made them represent the respective values of each points.

CHAPTER 3 RESULTS

3.1 General Explanation

The geochemical survey in the Eburru Prospect was conducted about four months between early 1980 and early 1982 and the number of stations surveyed is compiled in Table III-1.

As shown in Table III-1, in the Northern area six survey lines (L to Q) were set, in the Central area six lines (F to K) were set, and in the Southern area (A to E) were set.

There are some survey stations at which the field survey could not carry out because of unsuitable natural condition for the survey. The most common condition of this difficulty is caused by outcrop of hard igneous rocks, and in this case no small diameter hole could be dug. Therefore, the sampling of soil air and soil and the measurement of ground temperature at 1 meter deep from the landsurface were impossible.

The N-S interval of the survey line is closer in both the Northern and Southern areas compared to that of in the Central area, and hence, in the Central area the distributional patterns of each observed factor, like ground temperature and carbon dioxide, express more general trend.

3.2 1 Meter Depth Ground Temperature Measurement

The total number of stations where 1 meter depth temperature was measured is 827. The lowest ground temperature with 16.1 degree C was measured at the point A-29 locating at the west end of Eburru Crater with the altitude of 2,567 m above sea level.

The highest ground temperature with 93 degree C was measured at the point N-83 locating about 1,500 m southwest of Eburru Station with the altitude of 2,036.5 m above sea level. The highest elevation in all the survey stations is 2,718 m above sea level at the point E-140 locating about 2.2 km west of Eburru Peak, but the ground temperature at this point is not the lowest value.

The areal distribution of ground temperature is shown clearly the north-south trend, and this trend coincides well with the general trend of geological lineaments (faults).

The remarkable high temperature zones are distributed in both the Southern and Northern areas. In the Central area (F to K lines), high ground temperature is recognized in the western and the central parts, however, in those two parts the values of temperature (degree C) are lower than those in the Northern and Southern area.

The histogram of 1 meter depth ground temperature in the whole area is shown in Fig. III-3. The histogram is drawn based on the distributional trend in Fig. III-3, to clear up

the thermal characteristic in the whole area, we have decided to draw the equi-temperature lines of 20 degree C, 30 degree C, 40 degree C, etc. as expressed in Pl. III-2. The difference in elevation of the highest station and the lowest station reaches about 550 meters, thus, in the course of the compilation of the whole survey area, we must pay attention to the atmospheric temperature difference caused by the difference in altitude. According to US Standard Atmosphere 1976, the difference in average annual temperature between two stations which are about 550 m in altitude difference around 2,000 m above sea level is about four degrees Celcius. This matter is discussed in the next chapter.

3.3 Carbon Dioxide Content Measurement in Soil Air

At 827 survey stations, carbon dioxide content in soil air was measured. However, because strong microbial fermentation against recent organic matter was observed at the point N-109, the observed carbon dioxide content at the point was ignored. Thus the total number of effective stations is reduced to 826. The general trend of distribution of carbon dioxide in soil air for the whole survey area as well as for the individual three areas is shown in Table III-3 and Pl. III-3.

The histogram of carbon dioxide (%) in the whole area is shown in Fig. III-4.

The minimum value of carbon dioxide content in volume percent was 0.1, and this value was determined at many survey stations. The maximum values of carbon dioxide (%) were above 20, and the values were observed at the points A-22.0, A-22.5, B-18.5, and K-128.

In Table III-3 and Fig. III-4, the values above 0.5 % in carbon dioxide content may be recognized as anomalous values from geochemical point of view.

No relationship between the areal distribution of carbon dioxide in soil air and the vegetation on the landsurface was recognized.

General trend of carbon dioxide distribution in soil air is north-south direction.

The mean value of carbon dioxide in the three areas show that carbon dioxide concentration is highest in Southern area and lowest in Northern area. Values of carbon dioxide concentration vary most in Southern area and less in Central and Northern areas.

3.4 Mercury Concentration in Soil Air

Mercury concentration in soil air is measured in three different occasions, the first from January to February, 1980, the second from September to November, 1980, and the third from February to March, 1982. However, mercury values in soil air measured in the second phase are much lower than those of the other two phases. Therefore, on this report, data of only the first

and the third phases are used.

The general trend of distribution of mercury in soil air for the whole survey area as well as for the individual three areas is shown in Pl. III-4.

The histogram of mercury in nano gram per liter (ng/l) in the whole survey area is shown in Fig. III-5.

At over two third of the points, mercury content in soil air was less than the sensitivity of the mercury spectrometer which is about 0.15 ng/l. The maximum value of mercury content in the area was 22.5 ng/l and was determined at the points L-83, M-86 and P-121.

Concerning the general tendency of the distribution of mercury in soil air, the distributional trend is north-south, and the average value of mercury concentration in the Northern area and the Southern area is higher than that of in the Central area.

3.5 Mercury Concentration in Soil

Mercury concentration in soil was analyzed at 430 stations. The maximum mercury concentration value in soil is 6.7 ppm and its minimum value is 0.01 ppm. The maximum value is determined at the point B-25.0 at the caolinite clay pit and the minimum values are determined at many survey stations, mostly in the Northern area.

The histogram of mercury concentration (ppm) in soil is shown in Table III-5. The mercury content in soil is the highest in the Southern area and the lowest in the Northern area. The standard deviation shows that the mercury content in soil varies most in the Southern area and least in the Central area and in the Northern area the standard deviation value is the middle.

CHAPTER 4 DISCUSSION

4.1 1 Meter Depth Ground Temperature

Distribution of 1 meter depth ground temperature of the whole survey area, namely the Northern area, the Central area, and the Southern area, is shown in Fig. III-3.

The histogram of 1 meter depth temperature for the respective three divisional areas of the whole survey area are shown in Fig. III-7, III-8, and III-9 based on the numbers shown in Fig. III-3.

Comparing these three figures, the followings can be pointed out. In the Northern area (L to Q lines) : No station with ground temperature below 17.5 degree C was recognized. The value of the ratio of "number of stations below 17.5 degree C to number of stations between 17.5 degree C and 22.5 degree C" is minimum (zero). Many stations of between 22.5 degree C and 27.5 degree C were recognized.

In the Southern area (A to E lines) : The value of the ratio of "number of stations below 17.5 degree C to the number of stations between 17.5 degree C and the number of stations between 17.5 degree C and 22.5 degree C" is maximum and about two to five.

In the Central area (F to K lines) : The distributional trend of the figure lower than 29.9 degree C is that of the combination of the Northern and Southern areas. The value of the ratio of "number of stations between 27.5 degree C and 32.5 degree C and that between 22.5 degree C and 27.5 degree C" is 0.301 and the lowest.

The mean ground temperature value in the Southern area is the lowest and that in the Northern area is the highest. The mean elevation of the Southern area is the highest and about 500 m higher than that of the Northern area. Thus, the mean ground temperature of each area depends upon its elevation.

4.2 Carbon Dioxide Content Measurement in Soil Air

In the whole survey area, the distribution of carbon dioxide content in soil air is shown in Table III-3. Three figures, Fig. III-10, III-11 and III-12, show the histogram of carbon dioxide content for the respective three divisional areas, the Northern, the Central, and the Southern areas. For the histogram of carbon dioxide content, it is more clearly shows the distribution of carbon dioxide content measurement in this survey area to use common logarithm of carbon dioxide values than to use percentage values themselves. Therefore the histograms show their common logarithm.

There are more points which show carbon dioxide content over 0.5% in the Central and the

Southern areas than in the Northern areas. The percentage of the points over 0.5 % of carbon dioxide content in all survey points are 34 % in the Southern area, 23 % in the Northern area.

It is believed, as a rule, that the area from which large amount of carbon dioxide is escaping has relatively high potential in geothermal and such area must be paid attention from the exploration viewpoint. However, because carbon dioxide is easily dissolved in water, carbon dioxide may not reach to the ground surface at and around the place where underground water is abundance.

The small scaled carbon dioxide distribution may be controlled by the faults (lineament) and the reason of the repeated distributional pattern of carbon dioxide along the north-south faults may be caused by the difference in carbon dioxide feeding from the depth and / or by the difference in permeability in the near surface points of the faults.

The interpretation of the data on 1 meter depth ground temperature and carbon dioxide content in soil air, led us to the assumption that the water table in the Central area is deeper than that in the Northern area. Moreover, the topography in the Northern and Central areas shows that general trend of underground water flow is from south to north.

According to the previous report by the UN expert (gas geochemical expert) we notice the following points:

- (1) Only in the Southern area and in the south part of the Central area, natural steam without air contamination (without oxygen) is recognized.
- (2) About 20 steam samples from the Northern area and from the northern half of the Central area have high air contamination, regardless the blowout strength of steam vents.
- (3) The carbon dioxide content in the no-contamination steam samples ranges approximately from 0.1 to 0.4 percent.

Standing on the data stated above, we suppose that the carbon dioxide content in steam from the reservoirs in the Southern area and the southern part of the Central area may be less than 0.4 percent. Furthermore, in the Central and Southern areas, natural steam may be reserved in the reservoirs with relatively shallow depth (less than several hundred meters deep), however, in the Northern area, hot water may be reserved in relatively shallow reservoirs.

In the Northern area, many lineaments (faults) with relatively large and small scale coincide with the distribution of carbon dioxide in soil air. The areal distribution pattern of carbon dioxide in the whole survey area is generally similar.

The coincidence, stated above, is important from the stand point of geology and geochemistry. Thus, studies on the stratigraphy for the young formation and on the history of faults

should be continued.

4.3 Mercury Content Measurement in Soil Air

In the whole survey area, the distribution of mercury content in soil air is shown in Table III-4. The figure, Fig. III-5, shows the histogram of mercury content in the whole survey area. The histogram shows that only at 47 stations mercury content in soil air is over 0.625 ng/l and at other stations it is near the minimum mercury content or lower than the mercury content which the mercury spectrometer can detect. Therefore, the histogram shows the largest sample number of samples at the left end and the number of samples decreases toward the right, the higher mercury content.

The plate, Pl. III-4, shows the mercury distribution in soil air in the whole survey area. From the plate it is clear that the anomalous values of mercury content in soil air are mostly in the Northern area and the Southern area. In the Central area, the mercury content in soil air over 0.7 ng/l is detected only at two points. Even if we consider the mercury content over 0.2 ng/l is anomalous, the anomalous area is very narrow and limited in a few places in the Central area.

The reasons of high mercury content in soil air are as follows :

- (1) Due to geothermal activity, large quantity of mercury vapor is being produced under the survey point.
- (2) There exist passes to bring mercury rich air from the inside of the ground.
- (3) Because mercury vapor can be absorbed by rocks and clays, mercury rich air should not have passed through either long distance in rock or good mercury absorbent, like clays.

If we follow the genetic model of Eburru Geothermal Area, Fig. 5, we can explain the reason why mercury content in soil air in the Northern and the Southern areas is high and it in the Central area is low.

At or around Eburru Crater, the Southern area, the heat source is right underneath and large amount of mercury is vaporized at the heat source.

Around Eburru Station, the Northern area, the hot under ground water table is near the ground surface, and mercury is vaporized at near the surface, even though its amount may not be so large as at Eburru Crater.

However, at the Central area, the hot ground water table is deeper from the ground surface and no heat source exists underneath. Therefore mercury concentration in soil air is much less than those at the Northern and Southern areas.

Fig. III-3 Histogram of 1 Meter Depth Ground Temperature in the Eburru Prospect

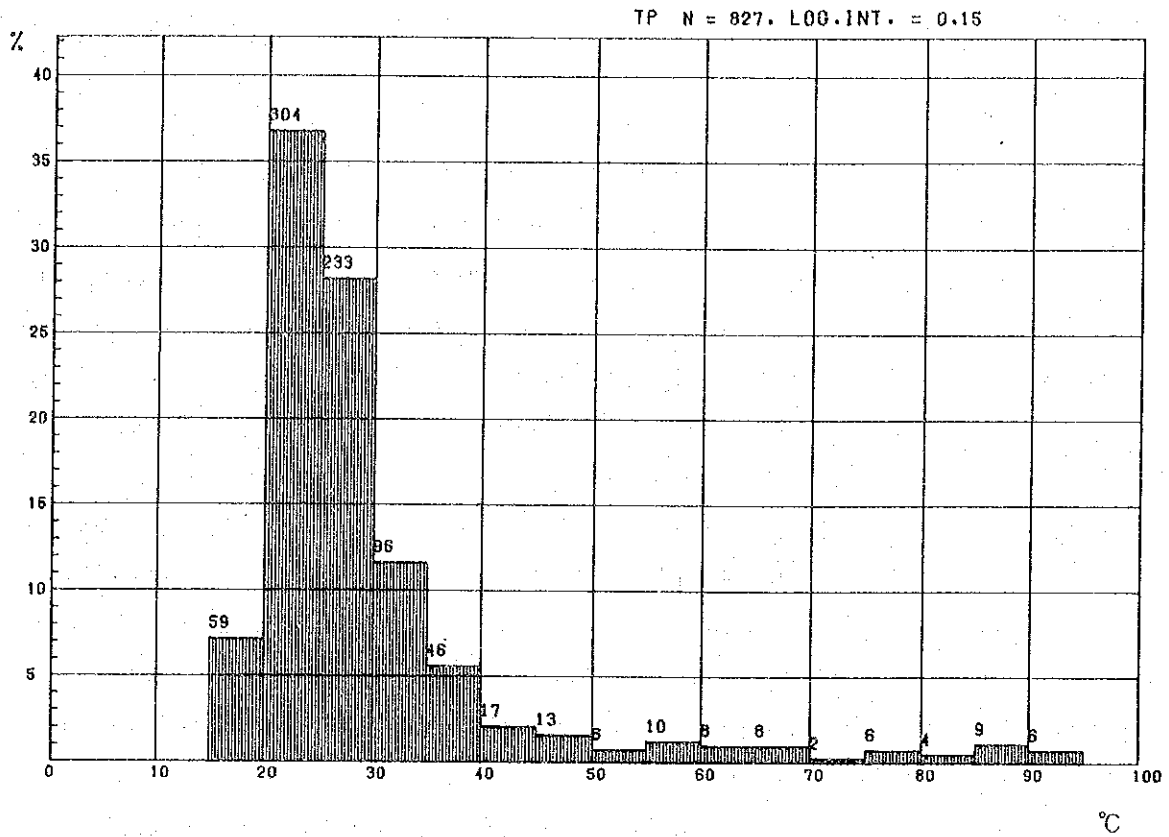


Fig. III-4 Histogram of Common Logarithm of CO₂ (%) in Soil Air in the Eburru Prospect

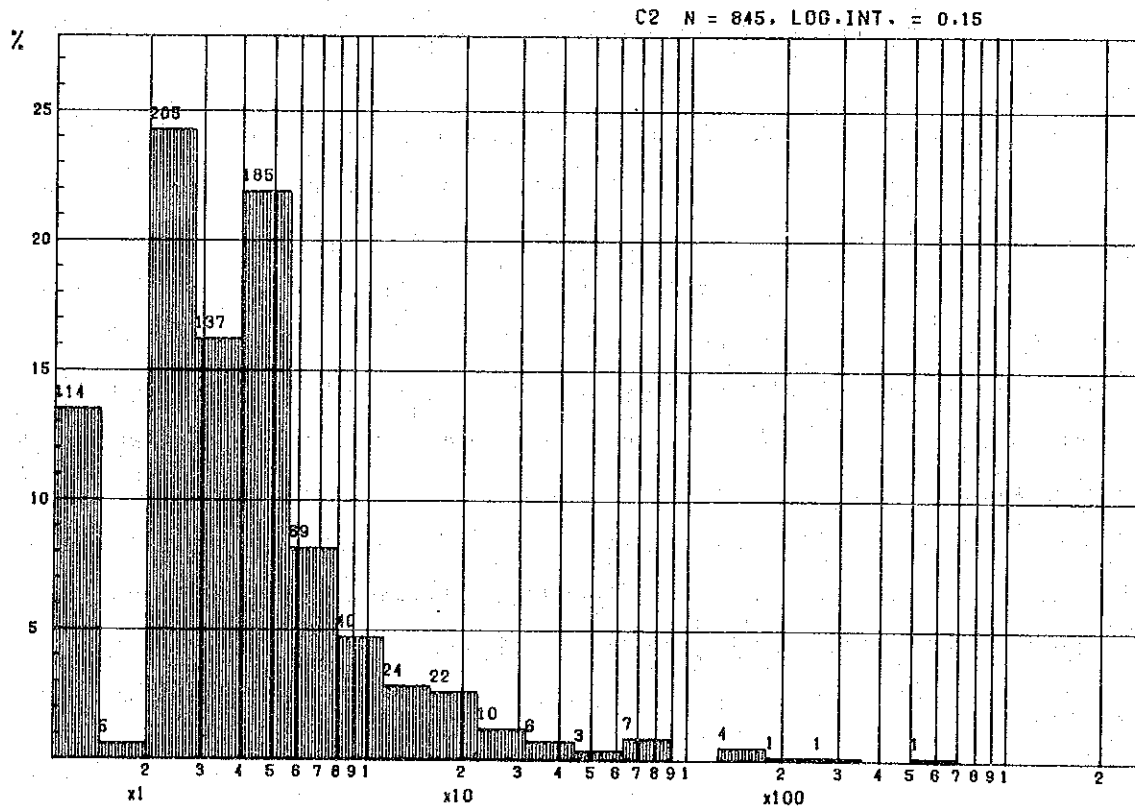


Fig. III-5 Histogram of Common Logarithm of Hg (ng/l) in Soil

Air in the Eburru Prospect

HA N = 439, LOG. INT. = 0.15

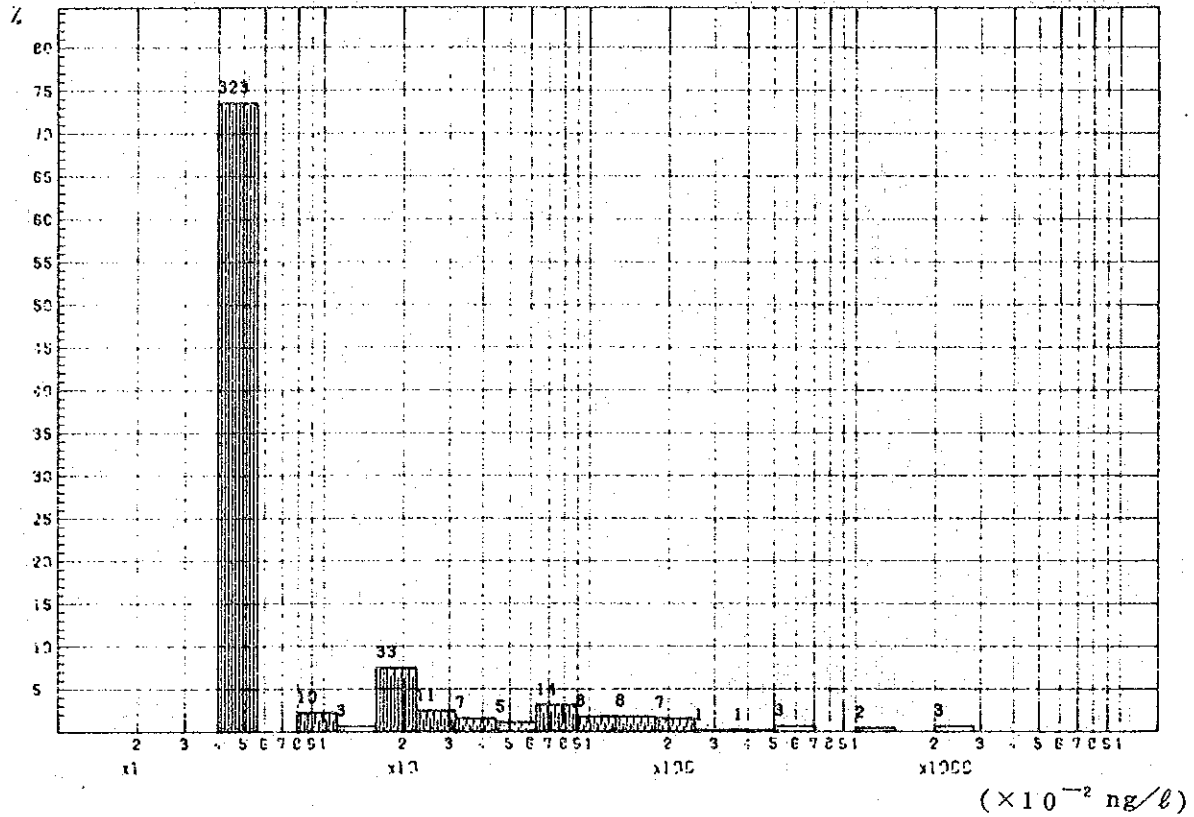


Fig. III-6 Histogram of Common Logarithm of Hg (ppm) in

Soil in the Eburru Prospect

HS N = 439, LOG. INT. = 0.15

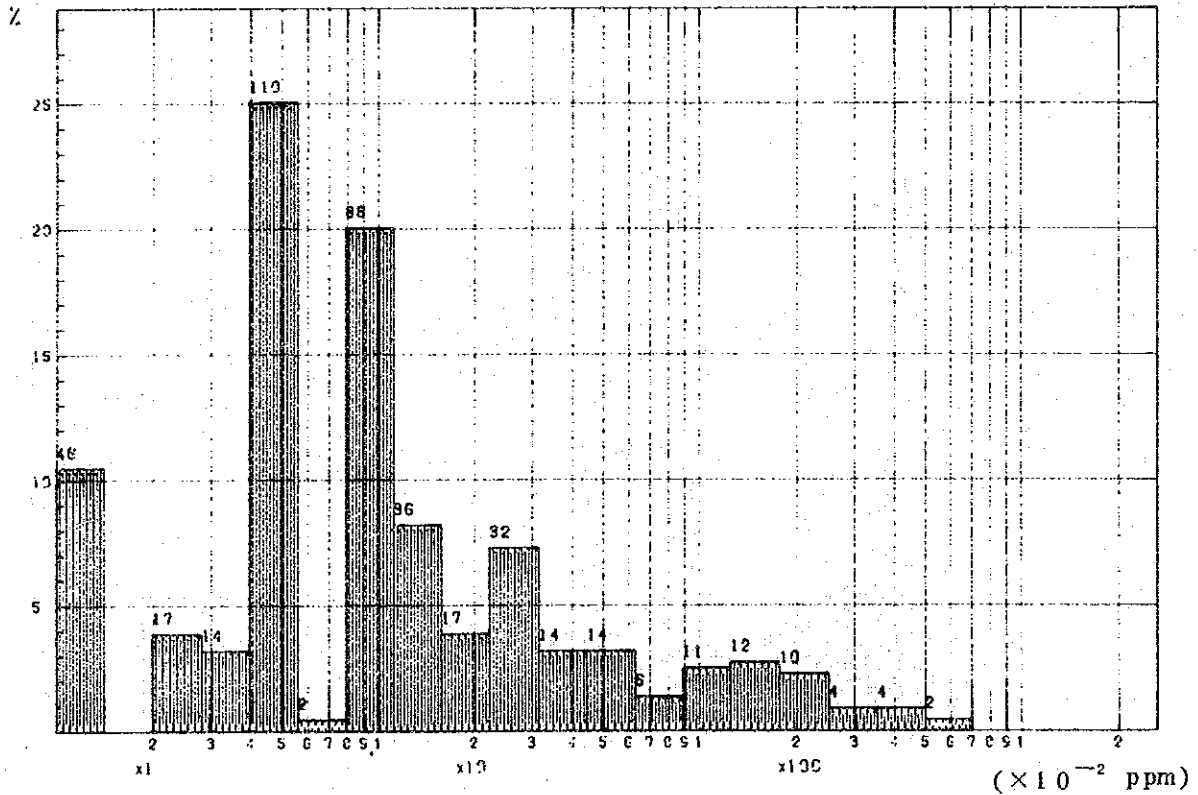


Fig. III-7 Histogram of 1 Meter Depth Ground Temperature in the Southern Area (line A to E)

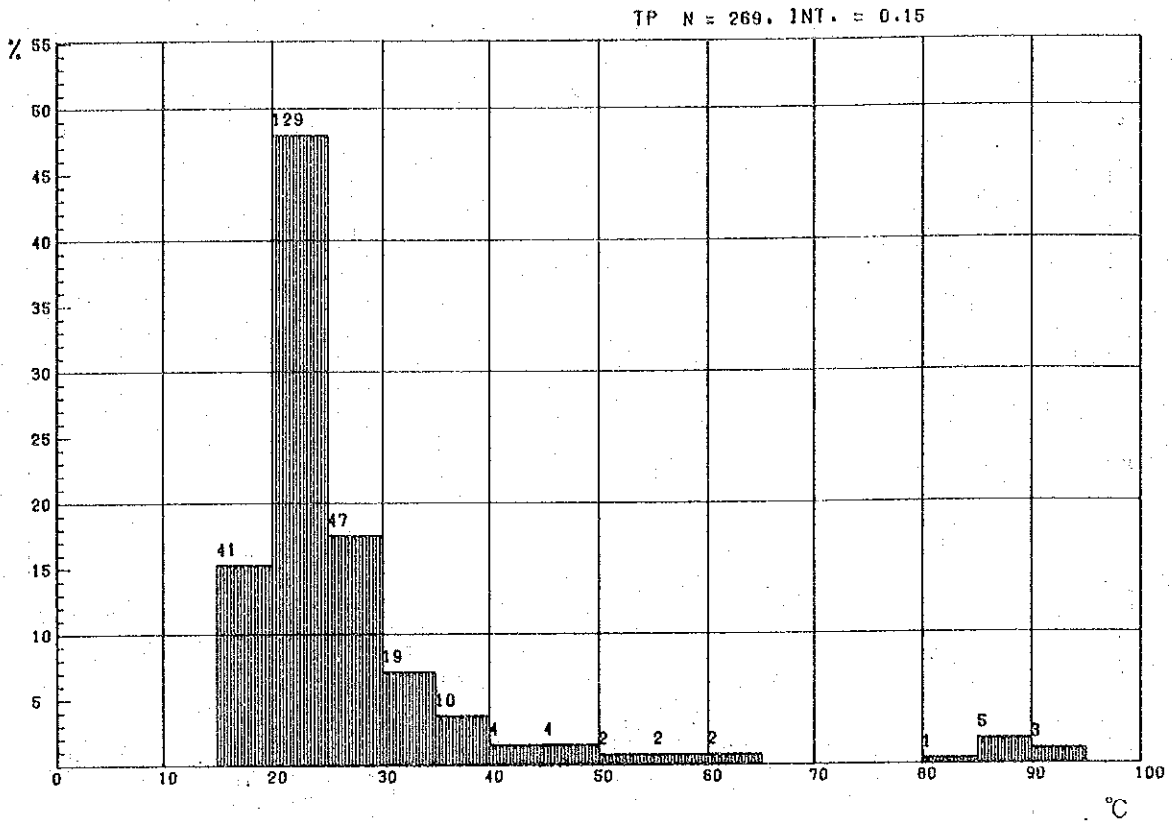


Fig. III-8 Histogram of 1 Meter Depth Ground Temperature in the Central Area (line F to K)

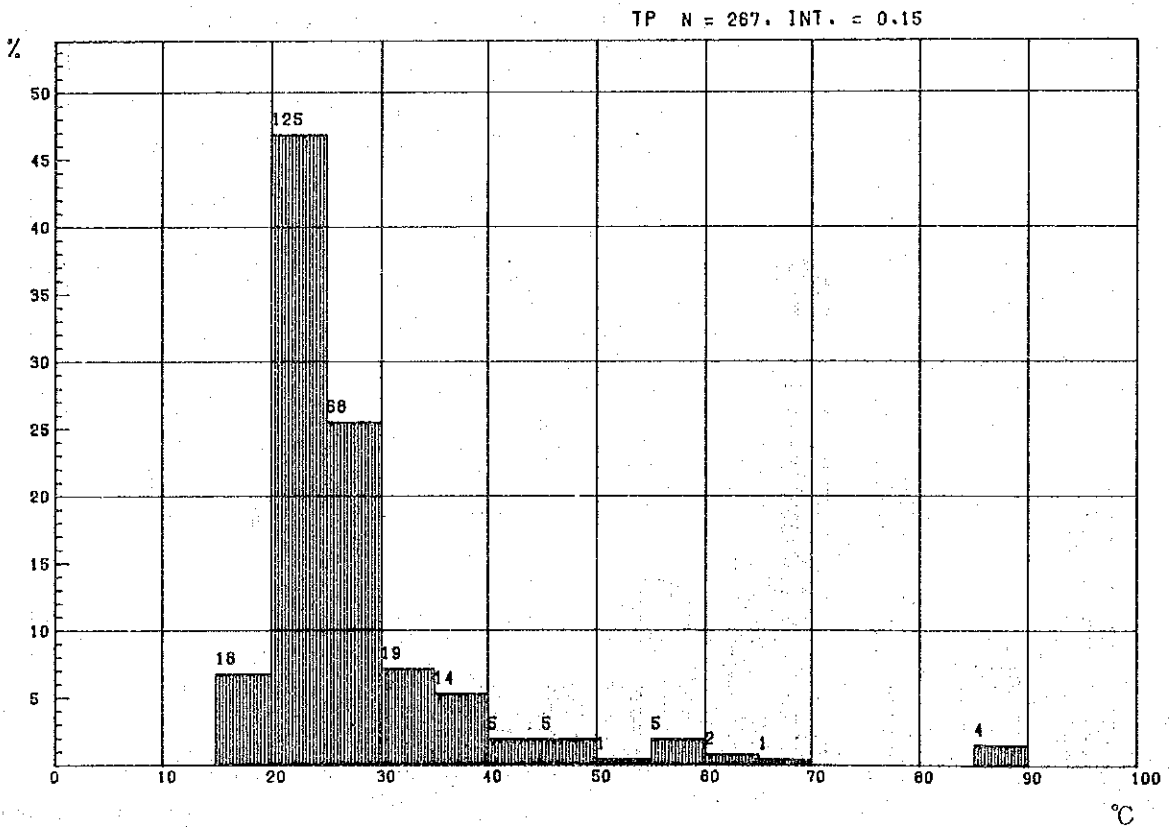


Fig. III-9 Histogram of 1 Meter Depth Ground Temperature
in the Northern Area (line L to Q)

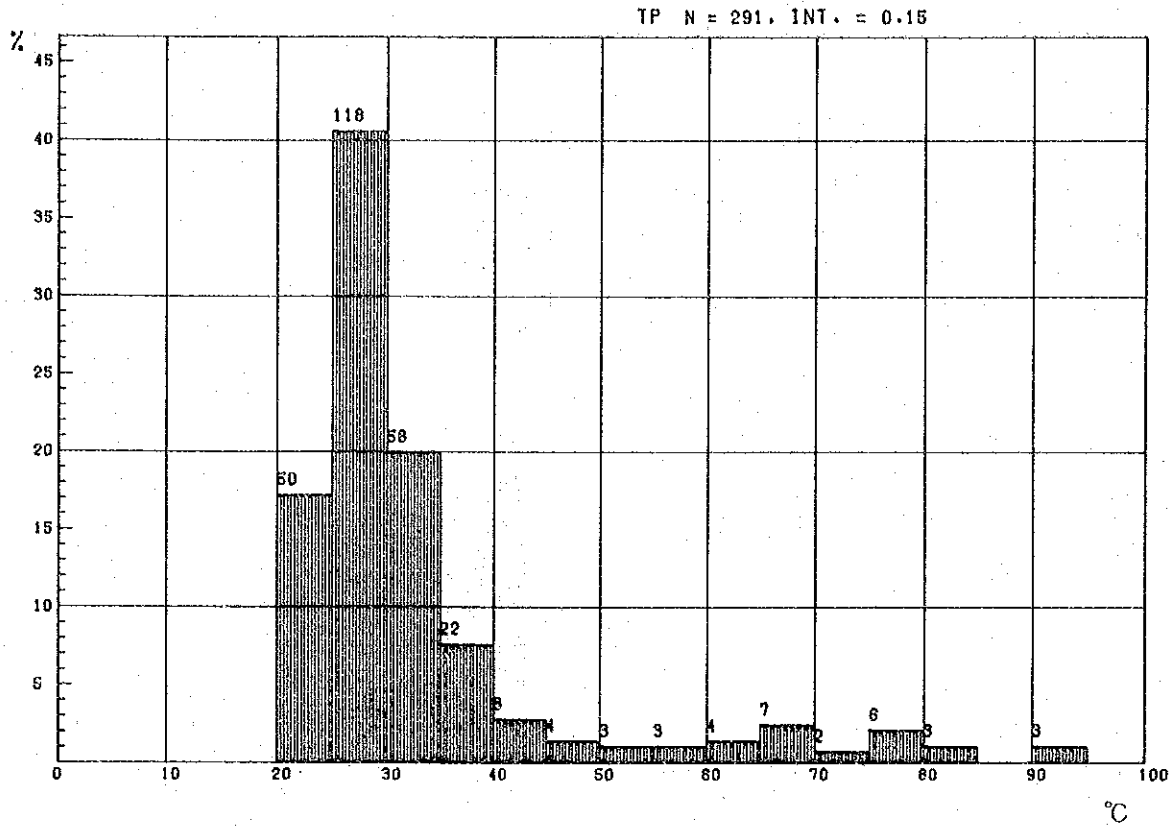


Fig. III-10 Histogram of Common Logarithm of CO₂ in Soil Air
in the Southern Area (line A to E)

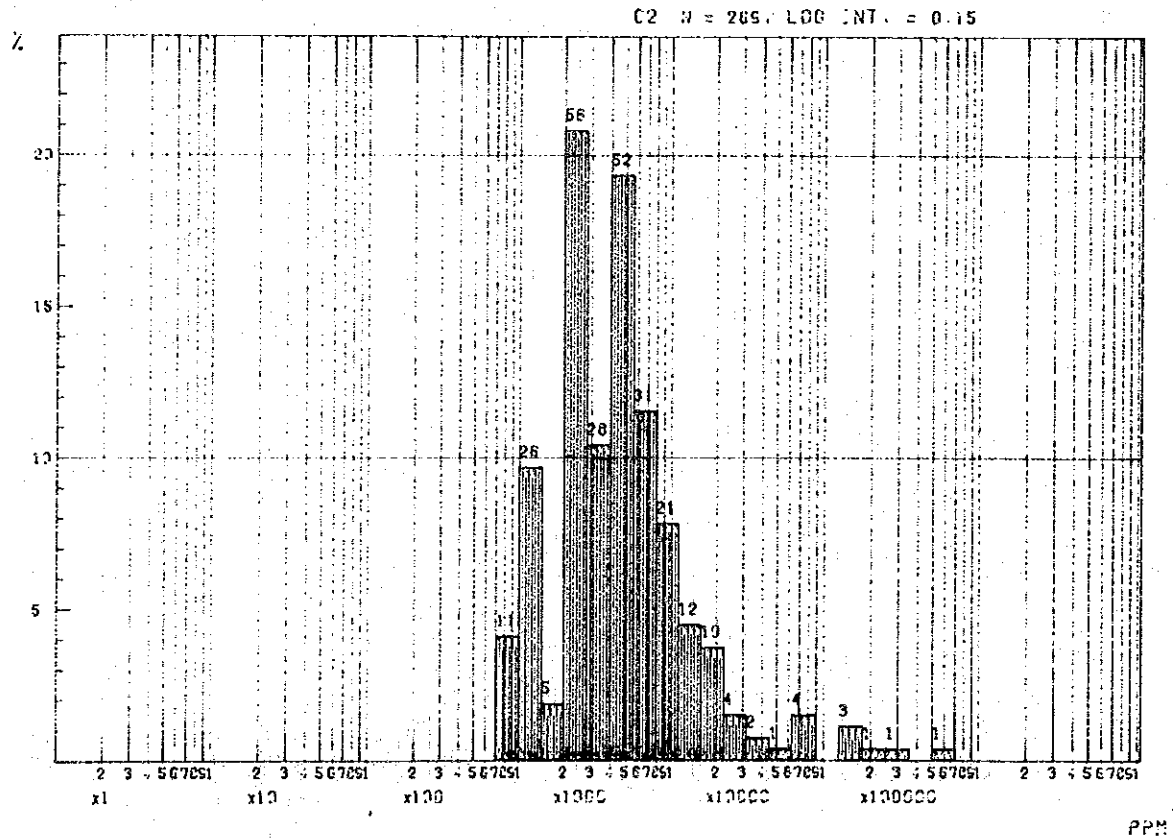


Fig. III-11 Histogram of Common Logarithm of CO₂ in Soil Air
in the Central Area (line F to K)

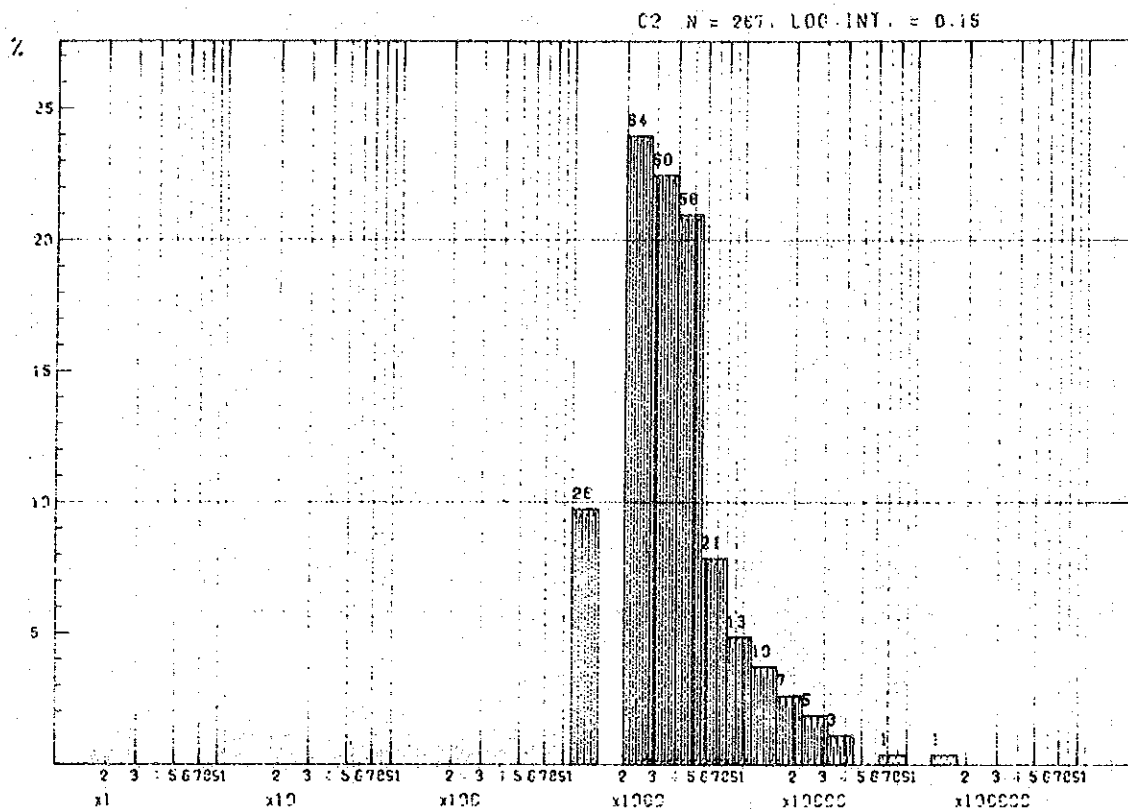


Fig. III-12 Histogram of Common Logarithm of CO₂ in Soil Air
in the Northern Area (line L to Q)

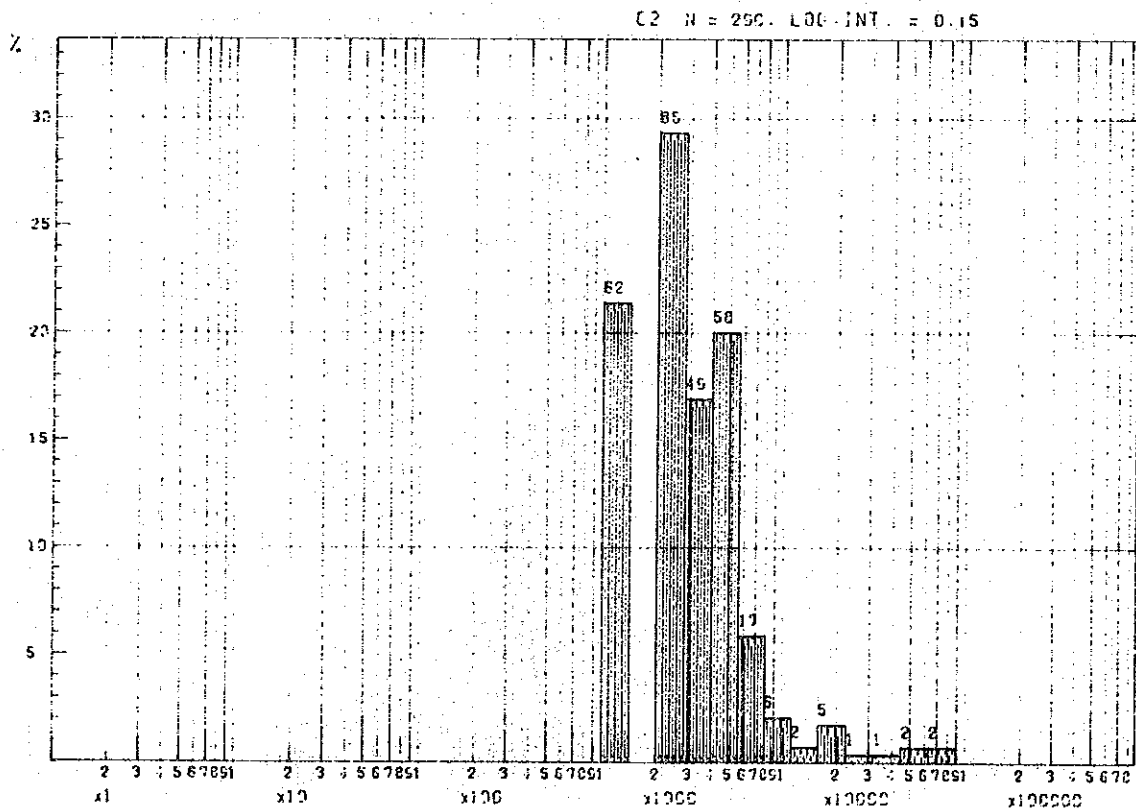


Table III-1 Survey Lines and Stations for Geochemical Survey in Eburru Prospect

Area	Line	No. of Stations	Line Length (km)	Ground Temp.	CO ₂ in Soil Air	Hg in Soil Air	Hg in Soil	Remarks
Northern Area	A	79	3.9	69	69			
	B	21	1.0	20	20			
	C	96	4.75	85	85			
	D	53	2.6	53	53			
	E	43	2.1	42	42			
Central Area	F	39	1.9	39	39			
	G	79	3.95	70	70			
	H	73	3.6	60	60			
	I	41	2.0	36	36			
	J	32	1.55	26	26			
Southern Area	K	40	1.95	36	36			
	L	49	2.40	37	37			
	M	62	3.05	52	52			
	N	53	2.60	48	47			
	O	59	2.95	47	47			
	P	56	2.75	47	47			
	Q	66	3.25	60	60			
	Total	863	42.30	827	826			

Table III-2 Histogram of 1 Meter Depth Ground Temperature

	Southern Area (line A - E)	Central Area (line F - K)	Northern Area (line L - Q)	Whole Area
12.5°C ~ 17.5°C	8	4	0	12
17.5 ~ 22.5	101	69	8	178
22.5 ~ 27.5	84	113	115	312
27.5 ~ 32.5	32	34	84	150
32.5 ~ 37.5	16	16	36	68
37.5 ~ 42.5	6	12	11	29
42.5 ~ 47.5	4	2	6	12
47.5 ~ 52.5	4	5	2	11
52.5 ~ 57.5	3	5	3	11
57.5 ~ 62.5	1	1	3	5
62.5 ~ 67.5	1	1	4	6
67.5 ~ 72.5	0	1	6	7
72.5 ~ 77.5	0	0	5	5
77.5 ~ 82.5	0	0	4	4
82.5 ~ 87.5	1	3	1	5
87.5 ~ 92.5	8	1	2	11
92.5 ~ 97.5	0	0	1	1
Total No.	269	267	291	827
Mean Value	27.6	27.9	33.4	29.7
S.D.*	13.8	11.1	14.1	13.4

* S.D.: Standard Deviation

Table III-3 Histogram of Common Logarithm of CO₂ Value in % in Soil Air

	Southern Area (line A – E)	Central Area (line F – K)	Northern Area (line L – Q)	Whole Area
-1.1 ~ -0.9 (0.079% ~ 0.126%)	37	26	62	125
-0.9 ~ -0.7 (0.126 ~ 0.20)	5	0	0	5
-0.7 ~ -0.5 (0.20 ~ 0.32)	81	124	134	339
-0.5 ~ -0.3 (0.32 ~ 0.50)	55	56	58	169
-0.3 ~ -0.1 (0.50 ~ 0.79)	31	21	17	69
-0.1 ~ 0.1 (0.79 ~ 1.26)	24	13	6	43
0.1 ~ 0.3 (1.26 ~ 2.0)	15	14	4	33
0.3 ~ 0.5 (2.0 ~ 3.2)	8	8	4	20
0.5 ~ 0.7 (3.2 ~ 5.0)	3	3	3	9
0.7 ~ 0.9 (5.0 ~ 7.9)	4	1	2	7
0.9 ~ 1.1 (7.9 ~ 12.6)	0	0	0	0
1.1 ~ 1.3 (12.6 ~ 20)	3	1	0	4
1.3 ~ 1.5 (20 ~ 32)	1	0	0	1
1.5 ~ 1.7 (32 ~ 50)	1	0	0	1
1.7 ~ 1.9 (50 ~ 79)	1	0	0	1
Total No.	269	267	290	826
Mean Value	-0.375 (0.422%)	-0.437 (0.366%)	-0.565 (0.272%)	-0.462 (0.345%)
S.D.*	0.488	0.366	0.348	0.411
A.M.V.**	1.228%	0.599%	0.432%	0.745%

* S.D.: Standard Deviation

** A.M.V.: Algebraic Mean Value

Table III-4. Histogram of Common Logarithm of Hg (ng/ℓ) in Soil Air

	Southern Area (line A – E)	Central Area (line F – K)	Northern Area (line L – Q)	Whole Area
0.079 n.g. ~ 0.126 n.g./ℓ	1	1	8	10
0.126 ~ 0.20	3	0	0	3
0.20 ~ 0.32	16	16	12	44
0.32 ~ 0.50	8	0	2	10
0.50 ~ 0.79	7	1	3	11
0.79 ~ 1.26	6	0	7	13
1.26 ~ 2.0	1	1	7	9
2.0 ~ 3.2	2	1	4	7
3.2 ~ 5.0	0	0	1	1
5.0 ~ 7.9	1	0	2	3
7.9 ~ 12.6	1	0	1	2
12.6 ~ 20	0	0	0	0
20 ~ 32	0	0	3	3
Total No. (A)	46	20	50	116
Mean Value	-0.321 (0.478 ng/ℓ)	-0.574 (0.267 ng/ℓ)	-0.163 (0.687 ng/ℓ)	-0.297 (0.505 ng/ℓ)
S.D.*	0.419	0.373	0.667	0.550
A.M.V.**	0.908	0.475	2.52	1.528
Stations less (B) than sensitivity	96	115	92	303
ratio of (A) and (B)	0.479	0.174	0.543	0.383

* S.D. : Standard Deviation

**A.M.V. : Algebraic Mean Value

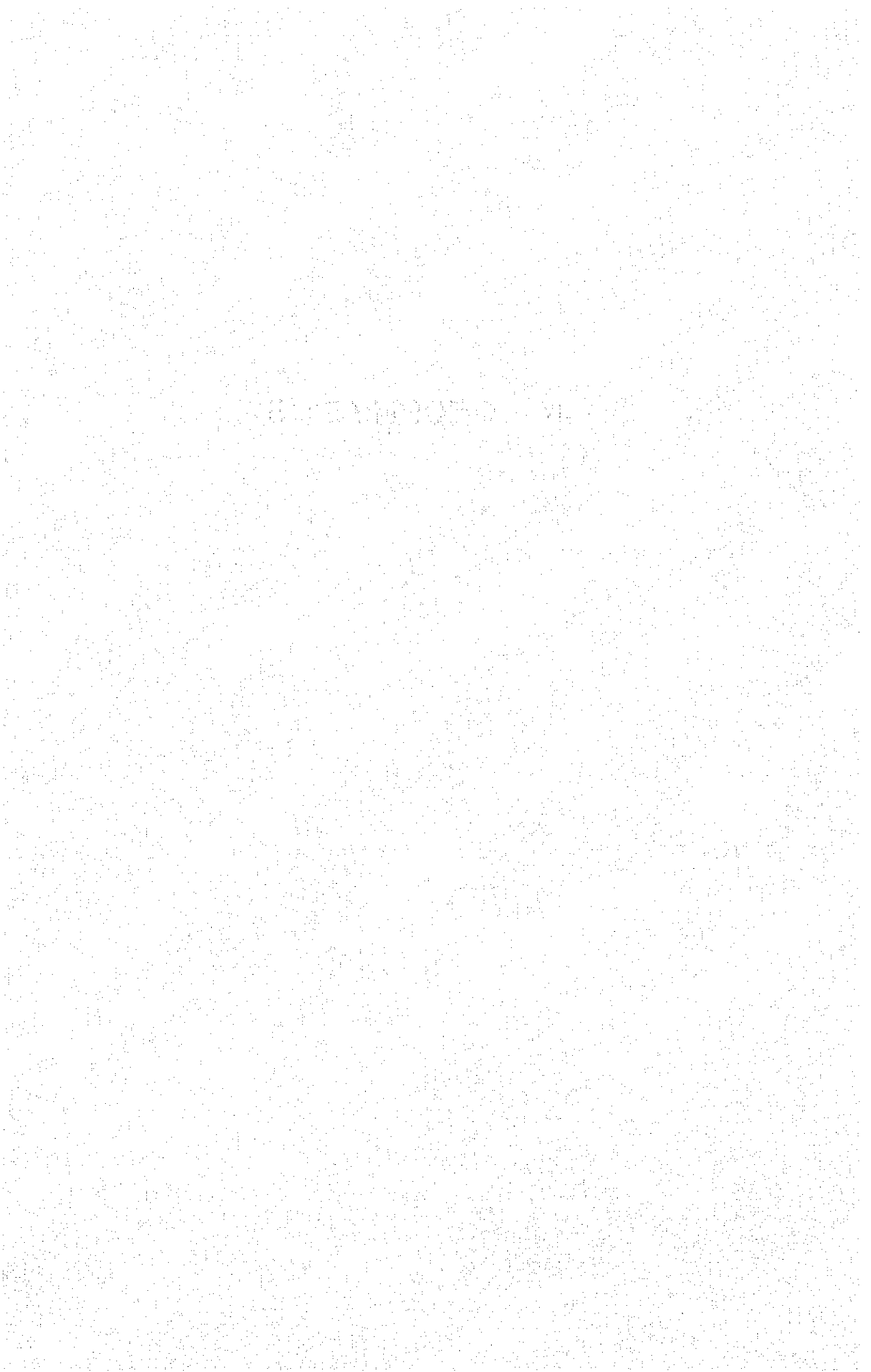
Table III-5 Histogram of Common Logarithm of Hg (ppm) in Soil

	Southern Area (line A - E)	Central Area (line F - K)	Northern Area (line L - Q)	Whole Area
0.0079 ppm ~ 0.0126 ppm	1	5	40	46
0.0126 ~ 0.020	0	0	0	0
0.020 ~ 0.032	0	10	21	31
0.032 ~ 0.050	5	38	67	110
0.050 ~ 0.079	0	2	0	2
0.079 ~ 0.126	43	30	15	88
0.126 ~ 0.20	11	20	5	36
0.20 ~ 0.32	20	24	5	49
0.32 ~ 0.50	14	4	1	19
0.50 ~ 0.79	7	3	1	11
0.79 ~ 1.26	15	0	0	15
1.26 ~ 2.0	10	2	3	15
2.0 ~ 3.2	8	0	0	8
3.2 ~ 5.0	6	0	1	7
5.0 ~ 7.9	2	0	0	2
Total No.	142	138	159	439
Mean Value	-0.492 (0.322ppm)	-1.024 (0.0946ppm)	-1.409 (0.0390ppm)	-0.991 (0.102ppm)
S.D.*	0.555	0.401	0.489	0.616
A.M.V.*	0.476 ppm	0.147 ppm	0.114 ppm	0.329 ppm

* S.D. : Standard Deviation

** A.M.V. : Algebraic Mean Value

IV . GEOPHYSICS



CHAPTER I INTRODUCTION

1.1 Relation Between Resistivity and Rocks

The relation between resistivity and rocks has been discussed by many people (Perkhomenko (1967), Keller and Frischknecht (1966)). Here it is reviewed after Keller and Frischknecht (1966).

Electrical conduction in near-surface rocks is almost entirely through the water filling pore-spaces in rocks. Conduction through mineral grains is important only in rare cases in near-surface rocks, such as where large concentrations of minerals such as magnetite, graphite or pyrrhotite are found, or at depth within the earth, where pore structure in the rock is closed by overburden pressure.

In water-bearing rocks, there is an indirect relation between resistivity and lithology or geologic age, since these two factors tend to control the porosity or water storage capacity of a rock, and to lesser extent, the salinity of the water contained in a rock.

A great deal of work has been done in correlating resistivity with water content for petroleum bearing rocks. For these rocks, which are primarily porous sandstones and limestones, it has been observed that resistivity varies approximately as the inverse square of the porosity and also the inverse square of the fraction of the pore space filled with water. The observation has led to the widespread use of an empirical function relating resistivity, porosity and water saturation which is known as Archie's law :

$$\rho_t = a S_w^{-n} \rho_w \phi^{-m}$$

where ρ_t is the bulk resistivity of the rock,

S_w is the fraction of the total pore volume filled with water,

ρ_w is the resistivity of the water contained in the pore structure,

ϕ is the porosity expressed as a fraction per unit volume of rock.

a , m and n are parameters whose values are assigned arbitrarily to make the equation fit a particular group of measurements

For a first approximation a value of 1 may be assumed for a and a value of 2 for m and n . The value for the parameter a varies from slightly less than 1 for rocks with intergranular porosity to slightly more than 1 for rocks with joint porosity. The exponent m is somewhat larger than 2 for cemented and well-sorted granular rocks and somewhat less than 2 for poorly sorted and

poorly cemented granular rocks.

Resistivity of water decreases when its salinity increases and also when temperature rises. Therefore, in geothermal reservoir at high temperature and highly saline pore water, resistivity becomes significantly lower than surrounding host rocks.

Distribution of resistivity in underground is very useful tool to explore distribution of geothermal reservoir.

1.2 Electrical Survey in Eburru

Electrical soundings with Schlumberger array have been carried out along 12 survey lines, total of 33.2 km and at 81 center points in the survey area. Centers of the electrical soundings are generally at every 250 m along survey lines and in some lines they are at every 500 m interval. All the survey lines lie in approximately east-west direction so that they are orthogonal to the general direction of geological structures in Rift Valley.

Each set of measurements is taken as a sounding and sounding centers are put every 250 m. Therefore geoelectrical profile of the survey lines can also be inferred from the data collected.

CHAPTER 2 FIELD WORK

The field geophysical survey was conducted in three occasions, February, 1980, October, and November, 1980 and February and March, 1982. During our field survey, the Eburru area was fairly dry and it rained only in the afternoon. However on February and November, 1980, it rained even morning hour. The crew worked only in the morning to avoid encountering rain and lightning or intense sunshine.

2.1 Instruments

Following instruments were used for the geophysical survey. By the middle of 1981, the identical set of geophysical equipments were donated by JICA to Ministry of Energy and the crew used the donated set of equipments on 1982 to train Kenyan counterparts.

(i) Transmitter	Yokohama Electronics Lab. Model L5202
Maximum Power	800v, 5A
Frequency	0.1 Hz to 5 Hz and D.C.
Wave Form	Time Domain and Frequency Domain
Weight	50 kg
(ii) Engine Generator	Shindaiwa Kogyo Model 2400
Output Power	2400 vA
Voltage	100v
Frequency	60 Hz
(iii) Recorder	Toa Electronics Model ERR-100A
Range	1 mv – 100v, 16 ranges
Accuracy	0.5% (full scale)
Input Impedance	2 M Ω

2.2 Field Procedure

The Schlumberger electrode configuration, which is most commonly used electrode configuration for electrical sounding, is used for the survey. In this configuration the four electrodes are positioned symmetrically along a straight line, the current electrodes on the outside and the potential electrodes on the inside. To change the depth range of the measurements, the current electrodes are symmetrically displaced outward while the potential electrodes, in general, are left

at the same position. However, when the ratio of the distance between the current electrodes to that between the potential electrodes becomes too large, the potential difference, between the potential electrodes becomes too small to be measured with sufficient accuracy. Therefore the potential electrodes also must be displaced outward to make signal larger. On the measurement the ratio of the distance between the current electrodes to that between the potential electrodes is tried not to be less than five to one. When the potential electrodes are displaced outward, measurements were carried out at two consecutive values of the potential electrodes spacing, combined with the same value of the current electrodes spacing, and repeat measurements for the same current electrodes spacing is also repeated at two consecutive values of the current electrodes spacing. This procedure provide a good information on the effect of the displacement of the potential electrodes upon measurement. Illustration of the Schlumberger electrode configuration is shown in Fig. IV-1 and the wiring of the equipments is shown in Fig. IV-2.

2.3 Data Reduction

Current and potential readings were recorded on two pen-recorders. At the field, data were reduced to apparent resistivities to check general agreement to the data collected previously. After coming back to the camp, recorded paper was read and data were reduced into apparent resistivities using following equation.

$$\rho_a = \pi \cdot \frac{\frac{(AB)^2}{2} - \frac{(MN)^2}{2}}{MN} \cdot \frac{\Delta V}{I} \quad (IV-1)$$

where ρ_a : apparent resistivity (Ωm)
 ΔV : potential difference (volt)
 I : transmitting current (ampere)

In the equation (IV-1), a geometric constant K is defined as follows:

$$K = \pi \cdot \frac{\frac{(AB)^2}{2} - \frac{(MN)^2}{2}}{MN}$$

The equation (IV-1) can be rewritten

$$\rho_a = K \cdot \frac{\Delta V}{I} \quad (IV-2)$$

In the equation (IV-2) the geometric constant depends only on geometry of electrode configuration.

The calculated apparent resistivities (ρ_a) were plotted against one half of current electrode

spacing (usually written as $AB/2$) on a log-log paper. The ρ_a vs $AB/2$ curves are used to be interpreted as a sequence of several resistivity layers.

2.4 Interpretation of Data

The collected Schlumberger data contain not only geological (more correctly geoelectrical) informations but also some topographical effects and other technical limitations as an error. Electrical measurements and topographical line cuts were carried out within an accuracy of around one percent. Therefore the collected apparent resistivity data may have a few per cent of measurement error.

There are many techniques being suggested to interpret Schlumberger resistivity sounding (see, for instance, Koefoed (1979), Keller and Frischknecht (1966)). All of these suggested techniques are based upon the assumption of horizontally layered earth and can be interpreted an apparent resistivity curve into a sequence of resistivity layers. In real survey we scarcely meet horizontally layered earth continuous down to several hundreds meters and laterally to a few kilometers where our assumption of horizontally stratified earth is valid to interpret an apparent resistivity curves.

On this report, curve matching technique was used to interpret all collected apparent resistivity data into sequences of horizontally stratified layers. Interpreted sequences of layers were put into a computer to get the theoretical apparent resistivity curves for each sequences. Thus obtained theoretical apparent resistivity curves were compared with the apparent resistivity curves from field operations.

Standard two-layer apparent resistivity curves and auxiliary graphs used for interpretation are published by Orellana and Mooney (1966).

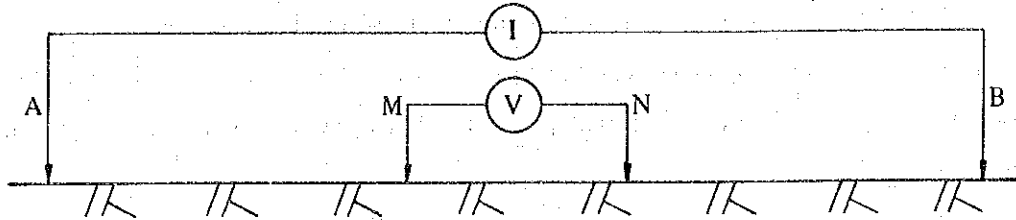


Fig. IV - 1 Schlumberger Electrode Configuration

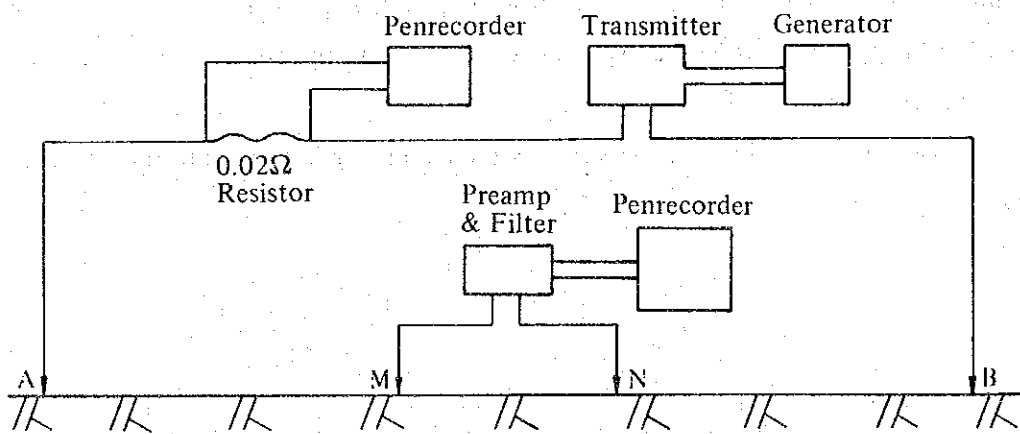


Fig. IV - 2 Wiring of Equipment

CHAPTER 3 RESULTS

Electrical depth soundings by Schlumberger electrode array have been carried out along 12 survey lines, namely, the lines A, B, C, D, E, H, I, K, M, O, P, and Q. They can be separated into three areas. The lines A, B, C, D, and E are in and around Eburru Crater (hereafter being called as Eburru Crater area), the lines H, I, and K are the north slope of Eburru Peak (hereafter being called as Cedar West Area), and the lines M, O, P, and Q are in the northern flat area around Eburru Station (hereafter being called as Eburru Station Area). Their locations are shown on Fig. IV-3.

Fig. IV-3 shows that the distribution of apparent resistivities at $AB/2 = 500$ m and suggests a general resistivity distribution in several hundreds meters deep in the ground. On Fig. IV-3, zone of apparent resistivity less than $20 \Omega\text{m}$ has a distribution only northern end and southern end of the area except a very small distribution at the center of the area along the line I. In the southern part of the area, Eburru Crater Area, apparent resistivity distribution is rather complicated. High apparent resistivity zone is only in the center of Eburru Crater and surroundings of Eburru Crater are dominated by lower apparent resistivity zones. In Eburru Crater Area, apparent resistivity distribution has a tendency to extend east-west direction.

In Eburru Station Area, apparent resistivity distribution tends to extend north-south direction which is the general direction of geological structures in the Rift Valley. Apparent resistivity zones of less than $20 \Omega\text{m}$ and between $20 \Omega\text{m}$ and $30 \Omega\text{m}$ occur intermittently. The algebraic means of the apparent resistivities at $AB/2 = 500$ m in Eburru Station Area are $33.7 \Omega\text{m}$ with the standard deviation of 20.2 along the line M, $31.9 \Omega\text{m}$ with the standard deviation of 16.7 along the line O, $28 \Omega\text{m}$ with the standard deviation of 13.3 along the line P, and $19.3 \Omega\text{m}$ with the standard deviation of 4.44 along the line Q. The algebraic means and the standard deviations along the lines M, O, P and Q show that the resistivity distribution at a few hundred meter deep along these lines tends to be lower and less variable toward north.

In Cedar West Area, both edges of the survey lines show high apparent resistivities and the middle part is dominated by lower apparent resistivities. Apparent resistivity distribution in Cedar West Area extends north-south direction. Lower apparent resistivity zone is in the center of a valley shape topography and the side walls of a valley shape topography are higher apparent resistivities.

Apparent resistivity pseudosections are drawn along eleven survey lines (see Fig. IV-5 (1) ~ (11)). Apparent resistivity pseudosections show general tendency of underground resis-

tivity structure.

The pseudosection along the line A show that high apparent resistivity zone upheaves at the center of Eburru Crater. Outside of the crater apparent resistivities are generally low. At the east end of the line A apparent resistivities are lower toward the depth.

The pseudosection along the line C shows that apparent resistivities along the line C are lower toward the depth. Especially around the outside of Eburru Crater, apparent resistivities are very low, as low as 9 Ωm .

The lowest apparent resistivity zone along the line D is between 200 m and 500 m below the surface of the ground and its resistivity value is between 10 Ωm and 20 Ωm . Near the surface of the ground high apparent resistivities are measured.

Along the line E, altitude is higher than other lines. Apparent resistivities are higher than other lines and have tendency to decrease toward deep. The lowest apparent resistivity measured is 21.2 Ωm .

Along the line H, equi-value lines of apparent resistivities are relatively horizontal. Apparent resistivities are lower toward the depth. Equi-value lines of apparent resistivities are uneven near the surface because of resistivity variation of the surface rocks.

Apparent resistivity pseudosection along the line I shows that low apparent resistivity at the center of the line and high apparent resistivity at the both sides.

Apparent resistivities along the line K are lower toward the east and lower toward the depth.

Apparent resistivities along the line M are lower toward the depth. At the point 105, apparent resistivities are higher than those of the both sides. The lowest apparent resistivity at the point 105 of the line M is 34 Ωm . On the other hand, it at the points 100 and 110 is less than 20 Ωm . At the east of the point 90, apparent resistivities are higher.

Apparent resistivity pseudosection along the line O shows that at the points 94 and 99 apparent resistivities are higher than those of the both sides. The lowest apparent resistivity at the points 89 and 104 is at around the deepest point and its value is less than 10 Ωm .

Apparent resistivity pseudosection of the line P shows that low apparent resistivity zone extends deep at the point 100 and the apparent resistivity value there is as low as 7.5 Ωm . At the surface of the point 100 it is over 1000 Ωm .

At the line Q, low apparent resistivity zone of apparent resistivity below 20 Ωm extends west of the station 100 and its value is lower toward the depth.

**Table IV -- 1 Statistics of Apparent Resistivities
at AB/2 = 500 m**

Line	Number of Stations	Mean	Standard Deviation
A	11	37.6 Ω m	27.1
B	1	20.1	—
C	6	17.8	4.60
D	6	16.6	3.13
E	5	36.0	6.20
H	9	29.0	4.74
I	3	96.4	72.7
K	5	34.9	13.0
M	9	33.7	20.2
O	7	31.9	16.7
P	6	28.0	13.3
Q	10	19.3	4.44
All	78	31.9	23.7

